Spatio-Temporal Theory of Optical Kerr Nonlinear Instability

Thesis submitted to the

Faculty of Graduate and Postdoctoral Studies

In partial fulfillment of the requirements for the degree:

Master of Science in Physics

Ottawa-Carleton Institute of Physics

Department of Physics

Faculty of Science

Author:

Michael J. Nesrallah

Supervisor:

Dr. Thomas Brabec

January 22, 2016

University of Ottawa

Abstract

This work derives a nonlinear optical spatio-temporal instability. It is a perturbative analysis that begins from Maxwell's equations and its constituent relations to derive a vectorial nonlinear wave equation. In fact, it is a new theoretical method that has been developed that builds on previous aspects of nonlinear optics in a more general way. The perturbation in the wave equation derived is coupled with its complex conjugate which has been taken for granted so far. Once decoupled it gives rise to a second-order equation and thus a true instability regime because the wavevector can become complex. The solution obtained for the perturbation that co-propagates with the driving laser is a generalization to modulation and filamentation instability, extending beyond the nonlinear Schrödinger and nonlinear transverse diffusion equations[1][2]. As a result of this new mechanism, new phenomena can be explored. For example, the Kerr Nonlinear Instability can lead to exponential growth, and hence amplification. This can occur even at wavelengths that are typically hard to operate at, such as into far infrared wavelengths. This provides a mechanism for obtaining amplification in the far infrared from a small seed pulse without the need for population inversion. The analysis provides the basic framework that can be extended to many different avenues. This will be the subject of future work, as outlined in the conclusion of this thesis.

Acknowledgements

First and foremost, I want to thank my supervistor, Dr.Brabec, who patiently guided me every step of the way. I've learned more working with him than any number of courses could teach me. I appreciate all the time and attention he's given me, despite being extremely busy. The past three years have been an unforgettable opportunity, and I'm looking forward to working with him in the future.

I would like to thank Dr.Varin and Dr.McDonald for their support while working in Dr.Brabec's group. I would like to thank Dr.Arissian, Dr.Vampa, Dr.Hammond, and Dr.Corkum for their experimental insights. Lastly, I would like to thank Dr.Boyd for teaching an excellent course in Nonlinear Optics and for authoring an invaluable textbook.

For Celeste

Contents

List of Figures

1 Introduction

The goal of this thesis is to explain some effects of Kerr nonlinearity[3] from the basis of our Kerr Nonlinear Instability (KNI) theory. Furthermore, instability results in either exponential growth or decay, as will be evident in this thesis. This leads to the prospect of amplification of a small seed pulse in wavelength regimes that are challenging to reach with other lasing techniques. This amplification results from KNI, and does not require population inversion of the medium. This will be discussed further in Chapter 4. The analysis done in this paper will also provide a stepping stone for other theoretical work to be done in Kerr nonlinear optics. It is a good place to start because the analysis describes the onset of the effects to first order approximation that can be built upon in future work. To begin, a context will be given by describing the background of Kerr nonlinearity.

Kerr nonlinear optics is an extension to linear optics that includes a nonlinear index of refraction responding quadratically to an applied electric field. This is described mathematically by considering Taylor expansion of the polarization vector[3]:

$$\boldsymbol{P} = \varepsilon_0 \chi^{(1)} \boldsymbol{E} + \varepsilon_0 \chi^{(2)} \boldsymbol{E}^2 + \varepsilon_0 \chi^{(3)} \boldsymbol{E}^3 + ... \tag{1}$$

The $\mathcal{O}(\boldsymbol{E}^3)$ term gives rise to the Kerr nonlinearity, and we are not considering the second order term in the expansion which is the Pockels effect[4]. The second order term vanishes identically due to centrosymmetry[3]. Even if it doesn't, we can still directly study the effects of Kerr nonlinearity in noncentrosymmetric material[5]. Furthermore, we are interested in isotropic materials, so this reduces the general tensor $\chi^{(3)}$ to a scalar and $\boldsymbol{E}^3 = |\boldsymbol{E}|^2 \boldsymbol{E}$[3]. The polarization vector then becomes:

$$\boldsymbol{P} = \varepsilon_0 \chi^{(1)} \boldsymbol{E} + \varepsilon_0 \chi^{(3)} |\boldsymbol{E}|^2 \boldsymbol{E}. \tag{2}$$

This polarization vector is the basis for Kerr nonlinear optics. Examples of the effects that are due to Kerr nonlinearity include: self-focusing, self-phase modulation, modulation instability, and filamentation instability[1][3][6][7]. To start, we discuss the background information of these effects and what is already

known about them. After this, we discuss how KNI can explain these effects and go beyond them; for instance, the prospect of KNI amplification of a small seed pulse.

1.1 Background information: What is known

We begin by discussing the spatial Kerr nonlinear effect of self-focusing.

1.1.1 Self-Focusing

The polarization vector given by Eq.(2) leads to a refractive index of the form $n = n_0 + n_2 I$, where n_0 is the linear contribution to the refractive index that arises from a term containing the linear electric susceptibility, $1 + \chi^{(1)}$, and n_2 is the second-order nonlinear index of refraction that arises from the third-order electric susceptibility, $\chi^{(3)}$[3]. The intensity, I, is related to a monochromatic electric field amplitude, E, by $I = \frac{c\epsilon_0 n_0}{2} E^2$[8], where ϵ_0 is the vacuum electric permittivity. The E^2 contribution comes from the third-order term in Eq.(2). Since $n \propto I$, the index of refraction varies linearly with the intensity profile.

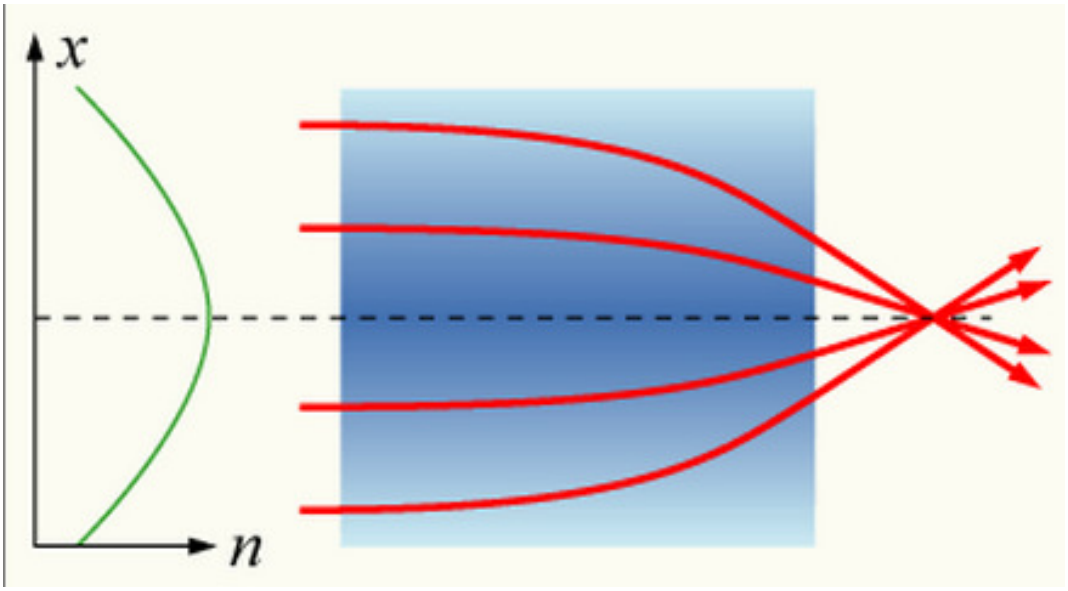

Figure 1: The transverse profile of the intensity of the laser leads to a transverse profile of the refractive index due to the kerr nonlinearity. This causes the beam to focus itself as it propagates through the nonlinear medium. *Courtesy of Wikimedia Commons, photonicswiki.org*

As seen in Fig. 1, in a typical laser beam profile where the intensity is highest in the middle, the refractive index is also highest in the middle, and hence there is a lens-like effect as the laser beam propagates through

the nonlinear medium. In most materials, n_2 is positive so the kerr nonlinearity acts as a positive lens, focusing in the material. Free electrons in the material can defocus the beam, acting like a negative lens. These effects are used to calculate the critical power required for self-focusing; if the pulse exceeds this critical input power so that it can overcome the natural diffraction that occurs in the medium and self-focusing will occur[3]. It is called 'self-focusing' because the laser beam is itself responsible for the focusing of the laser beam. As the laser beam propagates through the material, and if unhindered by any other process, this positive feedback loop occurs over and over until it collapses on itself. This either causes damage in the medium, or possibly the formation of plasma in gaseous materials, like air[9], which in turn defocuses the beam. This leads to a negative feedback loop of energy balancing. This can be considered a self-trapping of the laser. In reality, as well as a finite spatial profile, laser beams have a finite temporal profile. This means that the intensity is a function of time as well. This leads into the next Kerr nonlinear optical effect; self-phase modulation.

1.1.2 Self-Phase Modulation

Self-Phase Modulation (SPM) results from a time-dependent intensity profile, for then we have $n(t) = n_0 + n_2 I(t)$[3]. The time dependence in the refractive index translates to a phase shift in the pulse. This is because the wavevector is defined by $k = 2\pi n(t)/\lambda_0$, where λ_0 is the center wavelength, and the phase of the wave is given by $\phi(t) = \omega_0 t - kz = \omega_0 t - 2\pi n(t)/\lambda_0$, where ω_0 is the center frequency, and z is the propagation distance. The phase of the pulse then has the added time dependence from $n(t)$. This is especially significant in ultrashort pulses, because this leads to a significant instantaneous frequency shift, or chirp, of the pulse, given by $\omega(t) = d\phi(t)/dt = \omega_0 - 2\pi/\lambda_0 n_2 dI(t)/dt$[6].

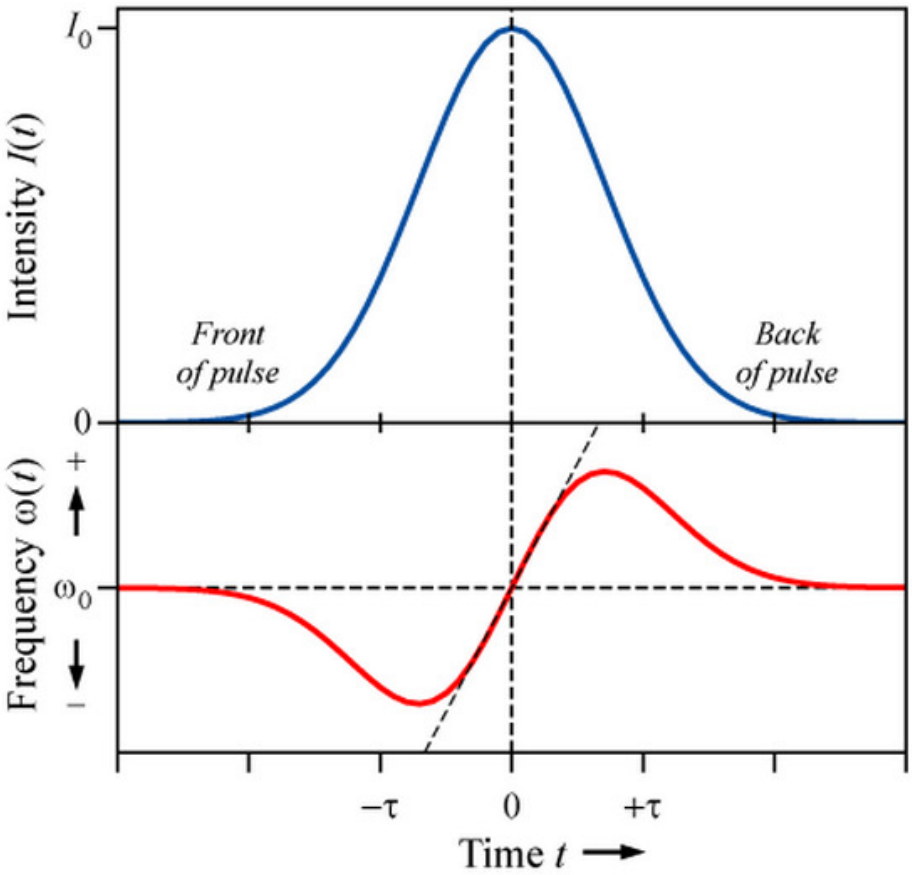

Figure 2: A temporal intensity profile gives rise to a temporal profile of instantaneous frequency. This results in a nonlinear phase shift due to kerr nonlinearity. The front of the pulse shifts to lower frequencies, and the back of the pulse to higher frequencies. Following the dashed lines, we see that the centre of the pulse has an approximately linear frequency shift. *Courtesy of Wikimedia Commons, http://commons.wikimedia.org/*

As seen in Fig. 2 additional frequencies that are generated by SPM broaden the spectrum symmetrically. The phase shift itself does not affect the temporal envelope of the pulse, but there is always group velocity dispersion (GVD)[1] that acts on the pulse simultaneously. In materials that exhibit normal dispersion the front of the pulse moves faster than the back, resulting in a broadening of the pulse in time and a compression of the pulse's frequency spectrum. Conversely, in materials that exhibit anomalous dispersion the front of the pulse moves slower than the back of the pulse, resulting in a compression of the pulse in time and a broadening of the spectrum. If the pulse is short enough in time, an equilibrium between SPM and anomalous GVD will result in a temporal soliton[10]. This means that the pulse will propagate remaining constant in both frequency and time. Consider, now, the first effect that arises directly from instability in a Kerr nonlinear medium; filamentation instability.

1.1.3 Filamentation Instability

The onset of filamentation instability is a result of small perturbations to the beam that transversely diffuse. Mathematically, one perturbs the electric field in the nonlinear transverse wave equation and finds the wavevector solution for the perturbation[2]. There is a transverse momentum space regime where the perturbations are stable with propagation, but there is also a regime where this instability occurs[2]. The KNI analysis that follows in this thesis will be a generalization to this in the appropriate limit, as is evident in Chapter 3.

Note that filamentation can occur in any dielectric, such as glass, air, or liquids[2]. In fact, the first evidence of filamentation was seen as filamentary damage tracks in glass[11]. Conversely, consider modulation instability, which is a temporal instability effect.

1.1.4 Modulation Instability

that arises from perturbations being reinforced by Kerr nonlinearity in the anom Modulation instability is a perturbation to a periodic waveform that is reinforced by nonlinearity. In the field of optics, modulation instability is usually studied within nonlinear fiber optics, the basis of which is taken from the Nonlinear Schrödinger equation (NLSE). Briefly, the NLSE is a wave equation that in this case relates the first-order longitudinal spatial derivative, the second-order derivative in time, the magnitude of which is characterized by group velocity dispersion, and the kerr nonlinear term that contains the electric field cubed. It is solved by introducing an ansatz of the form of a plane wave that is perturbed by a small function ε such that $\varepsilon^2 \approx 0$. The resulting first-order perturbation equation is obtained after inserting the ansatz and linearizing. An important detail is that after linearizing, one of the terms that results from the kerr nonlinearity is the complex conjugate of the perturbation, ε^*. This means that there is coupling between the perturbation and its conjugate, also between positive and negative frequency detunings, Ω and $-\Omega$. This is equivalent to a second-order equation that can be obtained by conjugating the linearized perturbation equation and decoupling.

A plane wave solution is readily obtained where the wavenumber of the perturbation is in the form of the square root of an argument due to the second-order nature of the wave equation that was derived. This

dispersion relation is strongly-dependent on the sign of the group velocity dispersion (GVD), β_2. One can Taylor expand the wavevector about the center frequency, ω_0 to obtain the power series $k = k_0 + \beta_1\Omega + \beta_2\Omega^2/2 + ...$, where $k_0 = k(\omega_0)$, $\beta_1 = k'(\omega_0)$ is the reciprocal of the group velocity, $\beta_2 = k''(\omega_0)$ is the group velocity dispersion, and so on[1]. If $\text{sgn}(\beta_2) = 1$, then we have normal dispersion and the wavenumber corresponds to oscillations around the unperturbed solution. However, if $\text{sgn}(\beta_2) = -1$, the argument under the square root can become negative, hence the wavenumber becomes imaginary and leads to instability in the form of exponential growth. The wavenumber is a dispersion relation meaning that it is a function of the frequency of perturbation, Ω. The maximum growth can be found by optimizing with respect to Ω, resulting in a positive and negative solution where maximum growth occurs, symmetrically about the center frequency ω_0.

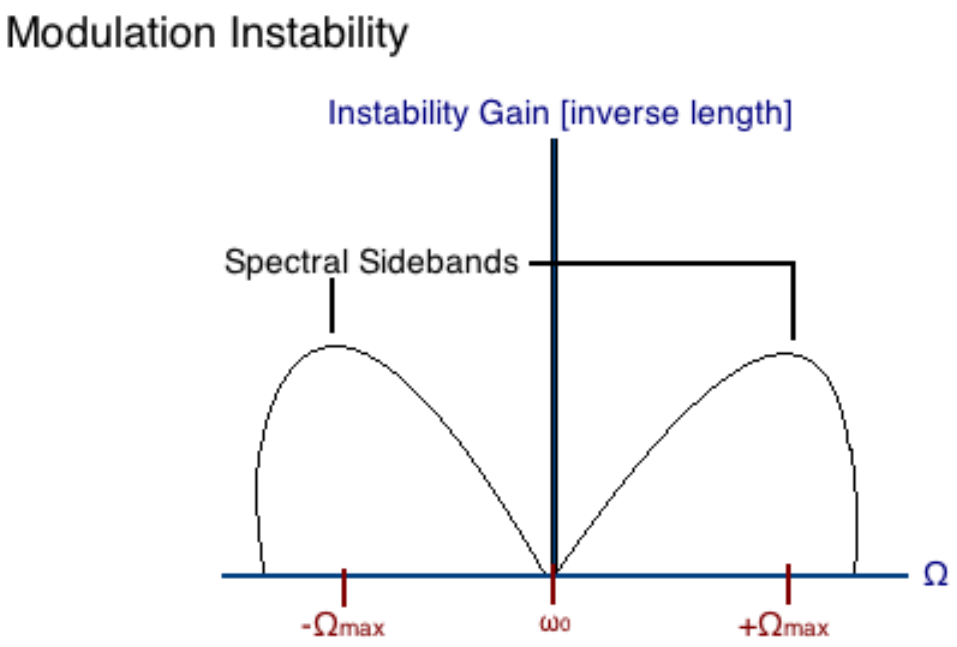

Figure 3: Modulation instability produces spectral sidebands from a perturbation when GVD is negative due to kerr nonlinearity. The instability is a gain to the perturbation that can amplify it to magnitudes comparable to the pump beam.

As seen in Fig. 3, these values for Ω_{max} explain the location of spectral sidebands, since this is where maximum growth occurs. Although not explained analytically by this first-order analysis, the sidebands can grow to become comparable in magnitude to the original delta-like peak that is from the continuous

wave and form their own sidebands. This process cascades, broadening out the spectrum. Now that this background information is established, let us examine how our theory of KNI can explain and generalize all these effects.

1.2 Kerr Nonlinear Instability

For tractability, the work of this thesis assumes that the driving laser field is a plane wave. Thus, the wave has infinite temporal and spatial extent. The plane wave (continuous wave) source implies a regime where dispersive effects, and self focusing effects are negligible. Dispersive effects are negligible for propagation distances $z \ll z_d$; $z_d = \tau_0^2/\beta_2$ is the dispersive length with τ_0 is the length of the pulse in time, and β_2 is the group velocity dispersion. Transverse self-action is weak as long as $z \ll z_{sf}$, where $z_{sf} = \mathrm{w_0}\sqrt{\mathrm{n_0}/(2\mathrm{n_n})}$ is the characteristic self focusing distance[3], where $\mathrm{w_0}$ is the pulse width.

Our perturbative spatio-temporal analysis will lead to a wavevector solution for the perturbation and the dispersion relation is a generalization to both filamentation and modulation instability. For instance, when we neglect the frequency dependence, but maintain the transverse components in our solution we obtain the filamentation instability limit. This provides good reinforcement of our model.

As for modulation instability, the main difference in our analysis is that we derive the vectorial perturbative wave equation which does not neglect transverse components. The spatio-temporal coupling gives rise to more physics, extending beyond modulation instability and filamentation. It will be shown that in the limiting case when we neglect the transverse wavevector and expand the refractive index in terms of group velocity and group velocity dispersion terms, we recover exactly what is obtained from the modulation instability analysis.

Beyond the above mentioned effects, KNI has the potential to be used as an amplifier in wavelength regimes that are not accessible with current laser technology. This will be discussed next.

1.2.1 Kerr Nonlinear Instability (KNI) Amplification

As will be evident in Chapter 4, in the appropriate parameter space of transverse wavevector and frequency detuning, the instability of perturbations to an electric field can result in exponential growth and decay

of the solutions. As outlined by filamentation and modulation instability, even a small perturbation to the input beam can grow by means of the Kerr nonlinearity of the medium, in the appropriate transverse momentum or dispersion regimes. The fact that the perturbing signal grows means that spatio-temoral coupling in Kerr media is technically a form of amplification. So far, this phenomenon has been considered in the limit of growing out of noise (the perturbation being noise), and leading to pulse break up. Here, we show that when a second seed pulse is added, KNI can act as an amplifier. By linearizing the perturbation, we explain the mechanism of amplification in a tractable, analytical way. This amplification results in very small perturbations of the signal to grow to the point of being comparable to the input signal itself, and beyond. For this work, our analysis is limited by linearization and the plane wave limit, and we can only describe the onset of amplification, without explicitly knowing how other effects, like SPM and self-focusing quantitatively effect the seed pulse. All we can do is assume propagation in a regime of appropriate length where these effects do not completely wash away the KNI amplification. Theoretically, the amplification of the perturbation can occur in common dielectric materials. However, it is advisable to choose materials with intrinsically higher nonlinear indices, such as Silver Gallium Selenide ($AgGaSe_2$)[12]. Furthermore, the amplification will be shown to outmatch absorption in a broad infrared (IR) wavelength range. This means that one could take the ordinary pump beam centered around, say, 800 nm and perturb it with a weak probe beam centered at a shorter or longer wavelength that could be amplified to an appreciable signal. In principle, this is a novel way to attain amplification in common materials at wavelengths that are harder to operate at, and without the need of population inversion within the lasing medium. This analysis will be done after we derive the appropriate second-order ordinary linear differential equation of the perturbation.

In the next chapter, we start with Maxwell's equations in order to derive the nonlinear wave equation. This spatio-temporal analysis demonstrates a different way of studying nonlinear optics. Thus, many of the mathematical details are included in the derivation to illustrate this method.

2 Spatio-Temporal Kerr Nonlinear Optics: The Derivation

We begin by deriving the paraxial linearized slowly evolving wave equation for the perturbation in the case where the source is a plane wave.

2.1 Perturbation Equation from Maxwell's Equations

The analysis is based on the nonlinear wave equation derived from Maxwell's equations. Specifically, Maxwell's equations in a Kerr medium. Using this form of the polarization vector we can now look at Faraday's and Ampère's laws and their constituent relations to derive the nonlinear wave equation that will form the basis of our analysis.

$$\boldsymbol{\nabla} \times \boldsymbol{E} = -\frac{\partial \boldsymbol{B}}{\partial t}, \tag{3}$$

$$\boldsymbol{\nabla} \times \boldsymbol{H} = \boldsymbol{J} + \frac{\partial \boldsymbol{D}}{\partial t}, \tag{4}$$

$$\boldsymbol{H} = \frac{1}{\mu_0}\boldsymbol{B}, \tag{5}$$

$$\boldsymbol{D} = \epsilon_0 \boldsymbol{E} + \boldsymbol{P}, \tag{6}$$

where $\boldsymbol{E}$ is the electric field, $\boldsymbol{B}$ is the magnetic flux density, $\boldsymbol{H}$ is the magnetic field, $\boldsymbol{J}$ is the current density, $\boldsymbol{D}$ is the electric flux denisty, μ_0 and ϵ_0 are the vacuum magnetic permeability and electric permittivity, respectively. As mentioned above, the electric polarization, $\boldsymbol{P}$, has both linear and nonlinear components, $\boldsymbol{P}^L = \varepsilon_0 \chi^{(1)} \boldsymbol{E}$ and $\boldsymbol{P}^{NL} = \chi^{(3)} \boldsymbol{E}^3$, where $\chi^{(1)}$ and $\chi^{(3)}$ are the first and third order electric susceptibilities, respectively. We are interested in isotropic materials, so this reduces $\chi^{(3)}$ to a scalar and $\boldsymbol{E}^3 = |\boldsymbol{E}|^2 \boldsymbol{E}$. The total polarization vector is then $\boldsymbol{P} = \varepsilon_0 \chi^{(1)} \boldsymbol{E} + \varepsilon_0 \chi^{(3)} |\boldsymbol{E}|^2 \boldsymbol{E}$. We can now use equations (3)−(6), to derive the wave equation. Taking the curl of equation (3) and using the vector identity $\boldsymbol{\nabla} \times \boldsymbol{\nabla} \times \boldsymbol{f} = \boldsymbol{\nabla}(\boldsymbol{\nabla} \cdot \boldsymbol{f}) - \boldsymbol{\nabla}^2 \boldsymbol{f}$,

we have:

$$\begin{aligned}\boldsymbol{\nabla}\times\boldsymbol{\nabla}\times\boldsymbol{E}(\boldsymbol{r},t) &= \boldsymbol{\nabla}(\boldsymbol{\nabla}\cdot\boldsymbol{E}(\boldsymbol{r},t)) - \boldsymbol{\nabla}^2\boldsymbol{E}(\boldsymbol{r},t) \qquad (7)\\ &= -\mu_0\frac{\partial}{\partial t}(\boldsymbol{\nabla}\times\boldsymbol{H}(\boldsymbol{r},t))\\ &= -\mu_0\left(\frac{\partial^2\boldsymbol{P}_i(\boldsymbol{r},t)}{\partial t^2}+\frac{\partial^2\boldsymbol{D}(\boldsymbol{r},t)}{\partial t^2}\right)\\ &= -\mu_0\frac{\partial^2}{\partial t^2}\left[\varepsilon_0\boldsymbol{E}(\boldsymbol{r},t)+\boldsymbol{P}(\boldsymbol{r},t)\right]\\ &= -\mu_0\varepsilon_0(1+\chi^{(1)})\frac{\partial^2\boldsymbol{E}(\boldsymbol{r},t)}{\partial t^2}-\mu_0\varepsilon_0\chi^{(3)}\frac{\partial^2}{\partial t^2}\left[|\boldsymbol{E}(\boldsymbol{r},t)|^2\boldsymbol{E}(\boldsymbol{r},t)\right]. \qquad (8)\end{aligned}$$

Using Eqs.(7) and (8) we arrive at the desired nonlinear wave equation in the time domain (with the space and time dependence implicitly understood):

$$\frac{\partial^2\boldsymbol{E}}{\partial z^2}+\boldsymbol{\nabla}_\perp^2\boldsymbol{E}-\boldsymbol{\nabla}(\boldsymbol{\nabla}\cdot\boldsymbol{E})-\frac{n^2*}{c^2}\frac{\partial^2\boldsymbol{E}}{\partial t^2}=\frac{\chi^{(3)}}{c^2}\frac{\partial^2}{\partial t^2}(|\boldsymbol{E}|^2\boldsymbol{E}). \qquad (9)$$

We have used the definition for the linear index of refraction, $n^2* = 1+\chi^{(1)}$, which is a convolution, or response function, with the electric field in the time domain. By the Convolution Theorem[13], the refractive index and electric field are thus multiplicative in the frequency domain. There is also the usual speed of light $c=\frac{1}{\sqrt{\varepsilon_0\mu_0}}$. Furthermore, we have split the Laplacian operator into its longitudinal (∂_z^2) and transverse ($\boldsymbol{\nabla}_\perp^2$) components. Although it is common to either neglect the $\boldsymbol{\nabla}(\boldsymbol{\nabla}\cdot)$ operator or write the wave equation in terms of a vector potential, we choose to derive the wave equation in terms of the electric field. Maintaining this term in Eq.(9) will yield a matrix equation in which the $\boldsymbol{x}$, $\boldsymbol{y}$, and $\boldsymbol{z}$ components are coupled.

It is natural to Fourier transform Eq.(9) so that we have multiplication of the refractive index and electric field instead of convolution. In Fourier space we also have algebraic expresisons instead of derivatives. Before this, though, let us insert the ansatz containing the perturbation, $\boldsymbol{E}=\Re\left\{\hat{\boldsymbol{x}}E_0e^{i\omega_0t-ik_0'z}+\boldsymbol{\varepsilon}(x,y,z,t)\right\}$, where $\Re\{\cdot\}$ denotes the real part of the argument, $\hat{\boldsymbol{x}}E_0e^{i\omega_0t-ik_0'z}$ describes the plane wave source polarized in the $\hat{\boldsymbol{x}}$ direction only, and $\boldsymbol{\varepsilon}(x,y,z,t)$ describes the generic perturbation to the source. Here, ω_0 is the center frequency of the laser field, $k_0'^2=k_0^2+\omega_0^2n_n/c^2$ is center wavenumber squared including the kerr nonlinearity, $k_0=\omega_0n_0/c$ is the usual wavenumber evaluated at the center frequency, and $\omega_0^2n_n/c^2$ is the

Kerr nonlinear contribution, with $n_n = \chi^{(3)} E_0^2$. We proceed in this regime by inserting the ansatz into Eq.(9):

$$\left[\partial_z^2 + \boldsymbol{\nabla}_\perp^2 - \boldsymbol{\nabla}(\boldsymbol{\nabla}\cdot) - \frac{n^2*}{c^2}\frac{\partial^2}{\partial t^2}\right]\left[\hat{\boldsymbol{x}} E_0 e^{i\omega_0 t - ik_0' z} + \boldsymbol{\varepsilon}(x,y,z,t)\right]$$

$$= \frac{\chi^{(3)}}{c^2}\frac{\partial^2}{\partial t^2}\left[\left|\left(\hat{\boldsymbol{x}} E_0 e^{i\omega_0 t - ik_0' z} + \boldsymbol{\varepsilon}(x,y,z,t)\right)\right|^2 \cdot \left(\hat{\boldsymbol{x}} E_0 e^{i\omega_0 t - ik_0' z} + \boldsymbol{\varepsilon}(x,y,z,t)\right)\right]. \tag{10}$$

The terms on the left-hand side of Eq.(10) acting on the plane wave source, together with the zeroth order terms on the right-hand side will vanish, as they should, because of the plane-wave ansatz that we used for $\boldsymbol{E_0}$. Consequently, the dispersion relation in the trial solution we imposed on $\boldsymbol{E_0}$ is valid for the zeroth-order equation because we are seeking the plane wave solution whereby the intensity, $I \propto E_0^2$, is constant. By evaluating $|\left(\hat{\boldsymbol{x}} E_0 e^{i\omega_0 t - ik_0' z} + \boldsymbol{\varepsilon}(x,y,z,t)\right)|^2 \left(\hat{\boldsymbol{x}} E_0 e^{i\omega_0 t - ik_0' z} + \boldsymbol{\varepsilon}(x,y,z,t)\right)$ the perturbation equation can be found. Writing for succinctness $\varepsilon(x,y,z,t) = \varepsilon$, explicitly we have:

$$\begin{aligned}&\left|\left(\hat{\boldsymbol{x}} E_0 e^{i\omega_0 t - ik_0' z} + \boldsymbol{\varepsilon}\right)\right|^2 \cdot \left(\hat{\boldsymbol{x}} E_0 e^{i\omega_0 t - ik_0' z} + \boldsymbol{\varepsilon}\right) \\ &= \left(E_0^2 + |\boldsymbol{\varepsilon}|^2 + E_0 \hat{\boldsymbol{x}} \cdot (\boldsymbol{\varepsilon^*} e^{i\omega_0 t - ik_0' z} + \boldsymbol{\varepsilon} e^{-i\omega_0 t + ik_0' z})\right) \cdot \left(\hat{\boldsymbol{x}} E_0 e^{i\omega_0 t - ik_0' z} + \boldsymbol{\varepsilon}\right).\end{aligned} \tag{11}$$

It is assumed that the perturbation is small enough such that only Kerr nonlinear terms oscillating with the fundamental frequency are kept and third harmonic terms are neglected; further, only contributions up to first order in $\boldsymbol{\varepsilon}$ are retained. This is a valid approximation for describing the onset of the effects that were discussed in Chapter 1. After expanding out Eq.(11) and linearizing in $\boldsymbol{\varepsilon}$ we obtain the following:

$$|\boldsymbol{E}|^2 \boldsymbol{E} = \hat{\boldsymbol{x}} E_0^3 e^{i\omega_0 t - ik_0' z} + E_0^2(\boldsymbol{\varepsilon} + \hat{\boldsymbol{x}}\varepsilon_x) + \hat{\boldsymbol{x}} E_0^2 \varepsilon_x^* e^{2i(w_0 t - k_0' z)}. \tag{12}$$

Inserting this into Eq.(10) and keeping in mind that the first term on the right hand side of Eq.(12) contributes to the zeroth-order equation that was discussed above, we obtain the linearized first-order perturbation equation:

$$\left[\partial_z^2 + \boldsymbol{\nabla}_\perp^2 - \boldsymbol{\nabla}(\boldsymbol{\nabla}\cdot) - \frac{n^2 *}{c^2}\frac{\partial^2}{\partial t^2}\right]\boldsymbol{\varepsilon} = \frac{n_n}{c^2}\frac{\partial^2}{\partial t^2}\left[\boldsymbol{\varepsilon} + \hat{\boldsymbol{x}}\varepsilon_x + \hat{\boldsymbol{x}}\varepsilon_x^* e^{2i(w_0 t - k_0' z)}\right]. \tag{13}$$

2.2 Transformation to the Fourier Domain

We make the transformation $\boldsymbol{\varepsilon}(\boldsymbol{x}, t) = \boldsymbol{u}(\boldsymbol{x}, t)e^{i\omega_0 t}$, where $\boldsymbol{x} = (x, y, z)$, and apply it to Eq.(13) to remove the carrier frequency from the perturbation. This will result in the frequency of the perturbation being an off-center detuning, $\Omega = \omega - \omega_0$.

As mentioned earlier, since the linear index of refraction, n, is a function of frequency, we have a convolution in the time domain. Transforming this equation into the Fourier domain, $\mathscr{F}[x, y, z, t] \mapsto [k_x, k_y, z, \Omega]$, we obtain a differential equation with respect to the longitudinal coordinate, z, only; with $n^2 * \boldsymbol{\varepsilon}(x, y, z, t) \mapsto n^2(\omega)\widetilde{\boldsymbol{u}}(k_x, k_y, z, \Omega)$. The Fourier transform is defined by

$$[\hat{F}(\boldsymbol{\varepsilon})](z, \mathbf{k}_\perp, \omega) = \frac{1}{(2\pi)^{3/2}}\int \mathrm{d}x\, \mathrm{d}y\, \mathrm{d}t\, \boldsymbol{\varepsilon}(\mathbf{x}, t)e^{-i(\omega t + \mathbf{k}_\perp \mathbf{r})}, \tag{14}$$

where $\mathbf{r} = (x, y)$ and $\mathbf{k}_\perp = (k_x, k_y)$ denote the transverse space and wavevector coordinates, respectively. We use the notation

$$[\hat{F}(\boldsymbol{\varepsilon})](z, \mathbf{k}_\perp, \omega) = [\hat{F}(\mathbf{u})](z, \mathbf{k}_\perp, \Omega) = \widetilde{\mathbf{u}}(z, \mathbf{k}_\perp, \Omega), \tag{15}$$

with the tilde symbol referring to a Fourier transformed field. The wave equation for the perturbation also contains a term with the Fourier transform of the complex conjugate of the perturbation field; this term is re-expressed as the complex conjugate of the Fourier transformed perturbation, i.e.,

$$\begin{aligned}&\hat{F}(\varepsilon_x^* \exp(2i\omega_0 t)) = [\hat{F}(u_x^*)](z, \mathbf{k}_\perp, \Omega) = \\ &[\hat{F}(u_x)]^*(z, -\mathbf{k}_\perp, -\Omega) = \widetilde{u}_x^*(z, -\mathbf{k}_\perp, -\Omega) = \widetilde{u}_{x(-)}^*.\end{aligned} \tag{16}$$

From now on, the notation, $\widetilde{u}_{x(-)}^*$, is used as a reminder that the complex conjugate of the Fourier transformed perturbation has to be evaluated at the negative frequency and transverse wavevector.

For clarity, before the above transformations are applied, the $\boldsymbol{\nabla}(\boldsymbol{\nabla}\cdot)$ operator from Eq.(13) can be explicitly calculated and expressed it in matrix form, rendering the task to be that of solving a matrix equation.

$$\boldsymbol{\nabla}(\boldsymbol{\nabla}\cdot) = \begin{pmatrix} \frac{\partial^2}{\partial x^2} & \frac{\partial^2}{\partial x \partial y} & \frac{\partial^2}{\partial x \partial z} \\ \frac{\partial^2}{\partial y \partial x} & \frac{\partial^2}{\partial y^2} & \frac{\partial^2}{\partial y \partial z} \\ \frac{\partial^2}{\partial z \partial x} & \frac{\partial^2}{\partial z \partial y} & \frac{\partial^2}{\partial z^2} \end{pmatrix}. \tag{17}$$

Applying the Fourier transform to this matrix, we have:

$$\mathscr{F}[\boldsymbol{\nabla}(\boldsymbol{\nabla}\cdot)] \equiv \widetilde{\mathbf{m}}\,(\widetilde{\mathbf{m}}\cdot) = \begin{pmatrix} -k_x^2 & -k_x k_y & ik_x\partial_z \\ -k_x k_y & -k_y^2 & ik_y\partial_z \\ ik_x\partial_z & ik_y\partial_z & \partial_z^2 \end{pmatrix}. \tag{18}$$

From now on, we use $\frac{\partial}{\partial z} \equiv \partial_z$ as the derivative operator for compactness. Applying the above operations in Eq.(13), the resulting vector wave equation for the perturbation is obtained as

$$\left(\partial_z^2 + k_z^2 - \widetilde{\mathbf{M}}\right)\widetilde{\mathbf{u}} = -\frac{n_n\omega^2}{c^2}\left(\widetilde{\mathbf{u}} + \hat{\boldsymbol{x}}\widetilde{u}_x + \hat{\boldsymbol{x}}\widetilde{u}^*_{x(-)}e^{-2ik_0' z}\right), \tag{19}$$

where $\widetilde{\mathbf{M}} = \widetilde{\mathbf{m}}\,(\widetilde{\mathbf{m}}\cdot)$ is the Fourier transformed gradient of divergence operator. Further, $k_z^2(\omega) = k^2(\omega) - k_\perp^2$, $k(\omega) = \omega n(\omega)/c$, and $k_\perp = (\boldsymbol{k}_\perp^2)^{1/2} = (k_x^2 + k_y^2)^{1/2}$, The vectorial nature that arises from $\widetilde{\mathbf{M}}$ causes the spatial components to be coupled. This will be evident if we explicitly expand out the system of equations arising because of $\widetilde{\mathbf{M}}$. Looking first at the equation for $\widetilde{u}_z$ from Eqs.(18) and (19) we have:

$$\begin{aligned} \partial_z^2\widetilde{u}_z + k_z^2\widetilde{u}_z - ik_x\partial_z\widetilde{u}_x - ik_y\partial_z\widetilde{u}_y - \partial_z^2\widetilde{u}_z + n_n\frac{\omega^2}{c^2}\widetilde{u}_z &= 0 \\ k_z^2\widetilde{u}_z + n_n\frac{\omega^2}{c^2}\widetilde{u}_z - ik_x\partial_z\widetilde{u}_x - ik_y\partial_z\widetilde{u}_y &= 0 \\ k_z'^{\,2}\widetilde{u}_z &= ik_x\partial_z\widetilde{u}_x + ik_y\partial_z\widetilde{u}_y \\ \widetilde{u}_z &= \frac{i}{k_z'^{\,2}}\partial_z\left(k_x\widetilde{u}_x + k_y\widetilde{u}_y\right), \end{aligned} \tag{20}$$

where $k_z'^2 = k'^2 - k_\perp^2$, and $k'^2 = k^2 + n_n\omega^2/c^2$. Since z is the longitudinal coordinate, Eq.(20) demonstrates that the second-order derivatives with respect to z cancel and thus $\widetilde{u}_z$ is not linearly independent from the $\widetilde{u}_x$ and $\widetilde{u}_y$ equations. We use Eq.(20) to eliminate the $\widetilde{u}_z$ terms that appear in the $\widetilde{u}_x$ and $\widetilde{u}_y$ equations that we will also derive from Eq.(19). Thus, it is sufficient to study the coupled transverse polarizations of the perturbation to get information about the whole system. Starting first with the $\widetilde{u}_x$ equation, and using Eqs.(19) and (20) we write:

$$\begin{aligned}
k_z'^2\widetilde{u}_x + k_x^2\widetilde{u}_x + \partial_z^2\widetilde{u}_x + k_xk_y\widetilde{u}_y - ik_x\partial_z\widetilde{u}_z &= -n_n\frac{\omega^2}{c^2}\left(\widetilde{u}_x + \widetilde{u}^*_{x(-)}e^{-2ik_0'z}\right)\\
\left(\partial_z^2 + k_x^2 + k_z'^2\frac{k_x^2}{k_z'^2}\partial_z^2\right)\widetilde{u}_x + \left(k_xk_y + \frac{k_xk_y}{k_z'^2}\partial_z^2\right)\widetilde{u}_y &= -n_n\frac{\omega^2}{c^2}\left(\widetilde{u}_x + \widetilde{u}^*_{x(-)}e^{-2ik_0'z}\right)\\
\left[\partial_z^2\left(1+\frac{k_x^2}{k_z'^2}\right) + k_x^2 + k_z'^2\right]\widetilde{u}_x + \left[k_xk_y\left(1+\frac{k_xk_y}{k_z'^2}\partial_z^2\right)\right]\widetilde{u}_y &= -n_n\frac{\omega^2}{c^2}\left(\widetilde{u}_x + \widetilde{u}^*_{x(-)}e^{-2ik_0'z}\right)\\
\left(k_x^2 + k_z'^2\right)\left(1+\frac{1}{k_z'^2}\partial_z^2\right)\widetilde{u}_x + k_xk_y\left(1+\frac{1}{k_z'^2}\partial_z^2\right)\widetilde{u}_y &= -n_n\frac{\omega^2}{c^2}\left(\widetilde{u}_x + \widetilde{u}^*_{x(-)}e^{-2ik_0'z}\right). \qquad (21)
\end{aligned}$$

Similarly for the $\widetilde{u}_y$ equation, we again look at Eqs.(19) and (20):

$$\begin{aligned}
k_z'^2\widetilde{u}_y + k_y^2\widetilde{u}_y + \partial_z^2\widetilde{u}_y + k_xk_y\widetilde{u}_x - ik_y\partial_z\widetilde{u}_z &= 0\\
\left(\partial_z^2 + k_y^2 + k_z'^2 + \frac{k_y^2}{k_z'^2}\partial_z^2\right)\widetilde{u}_y + \left(k_xk_y + \frac{k_xk_y}{k_z'^2}\partial_z^2\right)\widetilde{u}_x &= 0\\
\left[\partial_z^2\left(1+\frac{k_y^2}{k_z'^2}\right) + k_y^2 + k_z^2 + k_n^2\right]\widetilde{u}_y + \left[k_xk_y\left(1+\frac{k_xk_y}{k_z'^2}\partial_z^2\right)\right]\widetilde{u}_x &= 0\\
\left(k_y^2 + k_z'^2\right)\left(1+\frac{1}{k_z'^2}\partial_z^2\right)\widetilde{u}_y + k_xk_y\left(1+\frac{1}{k_z'^2}\partial_z^2\right)\widetilde{u}_x &= 0. \qquad (22)
\end{aligned}$$

We can summarize Eqs.(21) and (22) as a single matrix equation by recognizing the common factor of $\left(1+\frac{1}{k_z'^2}\partial_z^2\right)$ multiplying all the terms on the left-hand sides of the equations. Furthermore, we write $k_x^2 + k_z'^2 = k'^2 - k_y^2$, and $k_y^2 + k_z'^2 = k'^2 - k_x^2$. We then have:

$$\begin{pmatrix} k'^2 - k_y^2 & k_xk_y \\ k_xk_y & k'^2 - k_x^2 \end{pmatrix}\left(1+\frac{1}{k_z'^2}\partial_z^2\right)\begin{pmatrix} \widetilde{u}_x \\ \widetilde{u}_y \end{pmatrix} = \begin{pmatrix} -n_n\frac{\omega^2}{c^2}\left(\widetilde{u}_x + \widetilde{u}^*_{x(-)}e^{-2ik_0'z}\right) \\ 0 \end{pmatrix}. \qquad (23)$$

Now that the coupled differential equations of the linearized perturbation are in compact form, apply the

inverse matrix on the left-hand side of the equation to both left-hand sides of the equation. To be clear, we will explicitly calculate the inverse matrix, which is simple enough for a 2×2 matrix. First, calculate the determinant:

$$\begin{aligned}
\begin{vmatrix} k'^2 - k_y^2 & k_x k_y \\ k_x k_y & k'^2 - k_x^2 \end{vmatrix} &= (k'^2 - k_y^2)(k'^2 - k_x^2) - (k_x k_y)^2 \\
&= (k'^2)^2 + k_x^2 k_y^2 - (k'^2)(k_x^2 + k_y^2) - k_x^2 k_y^2 \\
&= (k'^2)(k'^2 - k_\perp^2) \\
&= k'^2 k_z'^2. \qquad (24)
\end{aligned}$$

Furthermore, we calculate the adjugate of the matrix:

$$\text{adj} \begin{pmatrix} k'^2 - k_y^2 & k_x k_y \\ k_x k_y & k'^2 - k_x^2 \end{pmatrix} = \begin{pmatrix} k'^2 - k_x^2 & -k_x k_y \\ -k_x k_y & k'^2 - k_y^2 \end{pmatrix}. \qquad (25)$$

Thus we can use the definition of the inverse of a 2×2 matrix, $\boldsymbol{A}$. That is, $\boldsymbol{A}^{-1} = \text{adj}(\boldsymbol{A})/\det(\boldsymbol{A})$. Applying this, we multiply on the left by the inverse matrix of Eqn.(23):

$$\left(1 + \frac{1}{k_z'^2}\partial_z^2\right) \begin{pmatrix} \widetilde{u}_x \\ \widetilde{u}_y \end{pmatrix} = -\frac{\omega^2}{c^2}\frac{n_n}{k'^2 k_z'^2} \begin{pmatrix} k'^2 - k_x^2 & -k_x k_y \\ -k_x k_y & k'^2 - k_y^2 \end{pmatrix} \begin{pmatrix} \widetilde{u}_x + \widetilde{u}^*_{x(-)} e^{-2ik_0' z} \\ 0 \end{pmatrix}. \qquad (26)$$

We multiply through by $k_z'^2$ and performing the matrix multiplication on the right-hand side of Eq.(26) we obtain:

$$\left(\partial_z^2 + k_z'^2\right) \begin{pmatrix} \widetilde{u}_x \\ \widetilde{u}_y \end{pmatrix} = -\frac{\omega^2}{c^2}\frac{n_n}{k'^2} \begin{pmatrix} k'^2 - k_x^2 \\ -k_x k_y \end{pmatrix} \left(\widetilde{u}_x + \widetilde{u}^*_{x(-)} e^{-2ik_0' z}\right). \qquad (27)$$

This can be further simplified by recognizing that $k'^2 = \frac{\omega^2}{c^2}\left(n^2 + n_n\right)$, and this coupled with the prefactor

$-\omega^2 n_n/(c^2 k'^2)$ reduces to $-n_n c^2\omega^2/[c^2\omega^2(n^2+n_n)] = -n_n/(n^2+n_n)$. Eq.(27) can now be written as:

$$\left(\partial_z^2 + k_z'^{\,2}\right)\begin{pmatrix}\widetilde{u}_x\\ \widetilde{u}_y\end{pmatrix} = -\frac{n_n}{n^2+n_n}\begin{pmatrix}k'^2 - k_x^2\\ -k_x k_y\end{pmatrix}\left(\widetilde{u}_x + \widetilde{u}^*_{x(-)}e^{-2ik_0' z}\right). \tag{28}$$

Notice that the $\hat{\boldsymbol{x}}$ equation is decoupled from $\widetilde{u}_y$. We then first solve the main equation, that of $\widetilde{u}_x$. This equation describes the part of the perturbation that copropagates with the driving laser, $\boldsymbol{E}_0$, and intuitively contains most of the energy. Hence most of the growth that can arise due to instability occurs for $\hat{\boldsymbol{x}}$-polarized light. This will be discussed below. However, the $\hat{\boldsymbol{y}}$ equation is non-vanishing due to the vectorial nature of the analysis, and hence growth of the perturbation can occur along $\hat{\boldsymbol{y}}$ as well. The solution of $\widetilde{u}_x$ can be inserted into the $\hat{\boldsymbol{y}}$-component of Eq.(28) for a full solution. For this thesis, the focus is on the $\hat{\boldsymbol{x}}$ equation. Subequent analysis will be the subject of future work. For now, rearranging the $\hat{\boldsymbol{x}}$ equation we have:

$$\begin{aligned}
&\left(\partial_z^2 + k'^2 - k_\perp^2 + \frac{n_n}{n^2+n_n}\left(k'^2 - k_x^2\right)\right)\widetilde{u}_x = -\frac{n_n}{n^2+n_n}\left(k'^2 - k_x^2\right)\widetilde{u}^*_{x(-)}e^{-2ik_0' z}\\
&\left[\partial_z^2 + \left(1+\frac{n_n}{n^2+n_n}\right)\left(k'^2 - k_x^2\right) - k_y^2\right]\widetilde{u}_x = -\frac{n_n}{n^2+n_n}\left(k'^2 - k_x^2\right)\widetilde{u}^*_{x(-)}e^{-2ik_0' z}\\
&\left\{\partial_z^2 + \left(1+\frac{n_n}{n^2+n_n}\right)\left[\frac{\omega^2}{c^2}\left(n^2+n_n\right) - k_x^2\right] - k_y^2\right\}\widetilde{u}_x = -\frac{n_n}{n^2+n_n}\left(k'^2 - k_x^2\right)\widetilde{u}^*_{x(-)}e^{-2ik_0' z}\\
&\left[\partial_z^2 + k''^2 - \left(1+\frac{n_n}{n^2+n_n}\right)k_x^2 - k_y^2\right]\widetilde{u}_x = -\frac{n_n}{n^2+n_n}\left(k'^2 - k_x^2\right)\widetilde{u}^*_{x(-)}e^{-2ik_0' z},
\end{aligned} \tag{29}$$

where $k''^2 = k^2 + 2\omega^2 n_n/c^2$. In this limit the asymmetry between transverse components, k_x and k_y, is neglected. The nonlinear refractive index is also small compared to the linear refractive index. Hence, terms $\propto n_n k_x^2$ are weak and can be neglected. This is a very good approximation for all natural optical materials. However, we would like to mention that in metamaterials it is possible to have the linear refractive index such that $n \leq 0$, for which these approximations break down. The materials of interest for this thesis are natural dielectric materials. Hence, we carry on with neglecting the transverse asymmetry arising from the vectorial

nature of Mawell's equations. This simplifies the analysis significantly, allowing for radial symmetry, so that

$$-\left[1+\frac{n_n}{(n^2+n_n)}\right]k_x^2-k_y^2\approx-(k_x^2+k_y^2)=-k_\perp^2;$$

eq.(29) then becomes:

$$\left(\partial_z^2+k_z''^2\right)\widetilde{u}_x=-\frac{n_n}{n^2+n_n}\left(k'^2-k_x^2\right)\widetilde{u}_{x(-)}^*e^{-2ik_0'z}, \tag{30}$$

where $k_z''^2=k''^2-k_\perp^2$. Now, we briefly turn our attention to the $\hat{\boldsymbol{y}}$-component of Eq.(28) to summarize the two equations that must be solved, in the above notation:

$$\left(\partial_z^2+k_z''^2\right)\widetilde{u}_x=-\frac{n_n}{n^2+n_n}\left(k'^2-k_x^2\right)\widetilde{u}_{x(-)}^*e^{-2ik_0'z}, \tag{31}$$

$$\left(\partial_z^2+k_z'^2\right)\widetilde{u}_y=\frac{n_n}{n^2+n_n}k_xk_y\left(\widetilde{u}_x+\widetilde{u}_{x(-)}^*e^{-2ik_0'z}\right), \tag{32}$$

continuing with the notation that $k_z'^2=k'^2-k_\perp^2$, and $k'^2=k^2+\omega^2n_n/c^2$.

2.3 Developing the Slowly Evolving Wave Equations

We proceed by looking at Eq.(31), and make use of the Slowly Evolving Wave (SEW) approximation[14]. The perturbation is split into a slowly evolving envelope and the rapidly oscillating plane wave with wavenumber $k_z''^2$ so that $\widetilde{u}_x=\widetilde{t}_xe^{-ik_z''z}$. We insert this into Eq.(31) and evaluate:

$$\begin{aligned}\left(\partial_z^2-2ik_z''\partial_z-k_z''^2+k_z''^2\right)\widetilde{t}_xe^{-ik_z''z}&=-\frac{n_n}{n^2+n_n}\left(k'^2-k_x^2\right)\widetilde{t}_{x(-)}^*e^{ik_z''z}e^{-2ik_0'z}\\ \left(\partial_z^2-2ik_z''\partial_z\right)\widetilde{t}_x&=-\frac{n_n}{n^2+n_n}\left(k'^2-k_x^2\right)\widetilde{t}_{x(-)}^*e^{2ik_z''z}e^{-2ik_0'z}.\end{aligned} \tag{33}$$

Under this approximation, the second-order longitudinal derivative of the slowly-evolving amplitude is negligible. Quantitatively, this is valid as long as $\left|\partial_z^2\widetilde{t}_x\right|\ll\left|2k_z''\partial_z\widetilde{t}_x\right|=$. Since $k''\propto\lambda_0$ to leading order, we have that the SEW approximation is valid provided that the variation of the perturbation over the extent of the center wavelength is negligible. Note that this approximation is not valid for appreciable frequencies

such that $\Omega/\omega_0 \gtrsim 1$[14]. However, it is used for the remainder of this work to illustrate the simplified theory of KNI, if we were to use the full wave equation without SEW it would prove to be too cumbersome as it deals with a fourth-order differential equation. Subsequent work can be done to solve the full equation to account for large frequency shift. For now, we continue with the SEW assumption and neglect the $\partial_z^2 \widetilde{t}_x$ term. This together with Eq.(33) gives

$$\partial_z \widetilde{t}_x = -\frac{i}{2k_z''} \frac{n_n}{n^2 + n_n} \left(k'^2 - k_x^2\right) \widetilde{t}^*_{x(-)} e^{2ik_z'' z} e^{-2ik_0' z}. \tag{34}$$

At this point, we transform back to $\widetilde{u}_x$ by using $\widetilde{t}_x = \widetilde{u}_x e^{ik_z'' z}$ and rearrange the SEW equation:

$$\begin{aligned}
\left(\partial_z + ik_z''\right) \widetilde{u}_x e^{ik_z'' z} &= -\frac{i}{2k_z''} \frac{n_n}{n^2 + n_n} \left(k'^2 - k_x^2\right) \widetilde{u}^*_{x(-)} e^{-ik_z'' z} e^{2ik_z'' z} e^{-2ik_0' z} \\
\left(\partial_z + ik_z''\right) \widetilde{u}_x &= -\frac{i}{2k_z''} \frac{n_n}{n^2 + n_n} \left(k'^2 - k_x^2\right) \widetilde{u}^*_{x(-)} e^{-2ik_0' z}.
\end{aligned} \tag{35}$$

We repeat this procedure for Eq.(32) to yield the the uniaxial propagation equations:

$$\left(\partial_z + ik_z''\right) \widetilde{u}_x = -\frac{i}{2} \frac{n_n}{n^2 + n_n} \frac{k'^2 - k_x^2}{k_z''} \widetilde{u}^*_{x(-)} e^{-2ik_0' z} \tag{36}$$

$$\left(\partial_z + ik_z'\right) \widetilde{u}_y = \frac{i}{2} \frac{n_n}{n^2 + n_n} \frac{k_x k_y}{k_z'} \left(\widetilde{u}_x + \widetilde{u}^*_{x(-)} e^{-2ik_0' z}\right). \tag{37}$$

Next we make the paraxial approximation $\mathbf{k}_\perp^2 / k'^2 \ll 1$, so that k_z' and k_z'' are readily Taylor expanded. Furthermore, we neglect the transverse wavevector components on the right hand side of Eqs.(36) and (37), keep only terms linear in n_n, as $n_n/n^2 \ll 1$, and neglect the nonlinear contribution to the transverse wavevector term. Further, from now on k' and k'' are Taylor expanded with respect to n_n to give

$$k^m(\omega) \approx k(\omega) + m k_n(\omega) \text{ with } k_n(\omega) = \frac{n_n k(\omega)}{2n^2(\omega)} \ ;$$

$$k^m = k', k'' \text{ for } m = 1, 2,$$

respectively. Using these approximations on the right-hand side of firstly Eq.(36) results in

$$\begin{aligned} -\frac{i}{2}\frac{n_n}{n^2+n_n}\frac{k'^2-k_x^2}{k_z''}\widetilde{u}^*_{x(-)}e^{-2ik_0'z} &\approx -\frac{i}{2}\frac{n_n}{n^2}\frac{k'^2}{k_z''}\widetilde{u}^*_{x(-)}e^{-2ik_0'z} \\ \approx -\frac{i}{2}\frac{n_n}{n^2}\frac{k^2}{\sqrt{k^2-k_\perp^2}}\widetilde{u}^*_{x(-)}e^{-2ik_0'z} &\approx -\frac{i}{2}\frac{n_n k}{n^2}\widetilde{u}^*_{x(-)}e^{-2ik_0'z} \\ &= -ik_n\widetilde{u}^*_{x(-)}e^{-2ik_0'z}. \end{aligned} \tag{38}$$

We have neglected the transverse components in Eq.(38) because otherwise it makes the subsequent analysis significantly more complicated, without noticeable benefit, as shown below in Fig. 4. The leading order term before conjugation, n_n, is assumed to be small and so after eliminating for the perturbation without its conjugate we will see that the leading order term on the right-hand side becomes n^2, so any transverse contributions become negligible. Similarly for the right-hand side of Eq.(37)

$$\begin{aligned} \frac{i}{2}\frac{n_n}{n^2+n_n}\frac{k_xk_y}{k}\left(\widetilde{u}_x+\widetilde{u}^*_{x(-)}e^{-2ik_0'z}\right) &\approx \frac{i}{2}\frac{n_n}{n^2}\frac{k_xk_y}{k_z}\left(\widetilde{u}_x+\widetilde{u}^*_{x(-)}e^{-2ik_0'z}\right) \\ \approx \frac{i}{2}\frac{n_nk}{n^2}\frac{k_xk_y}{k^2}\left(\widetilde{u}_x+\widetilde{u}^*_{x(-)}e^{-2ik_0'z}\right) &= i\frac{k_n}{k^2}k_xk_y\left(\widetilde{u}_x+\widetilde{u}^*_{x(-)}e^{-2ik_0'z}\right). \end{aligned} \tag{39}$$

The wavevector k'' of $\widetilde{v}_x$ contains double the nonlinear contribution of the wavevector k' of $\widetilde{v}_y$; this differences will manifest in various parameters with a nonlinear contribution throughout the following derivation. For all these cases we will use the same notation, $|^m = |', |''$ for $m = 1, 2$, indicating a difference of a factor of two in the nonlinear contribution. Further, we will use the Taylor expansion of k with regard to the frequency

$$k(\omega) = k_0 + D(\Omega), \tag{40}$$

with $D(\Omega) = \beta_1\Omega + (\beta_2/2)\Omega^2 + (\beta_3/6)\Omega^3 + \cdots$, where β_1 is group velocity term, β_2 is the group velocity dispersion, and β_3 is the third order dispersion, and so forth. When expanding the wavevectors containing

nonlinear terms, k' and k'', phase, group velocity and higher order terms D^m show nonlinear contributions,

$$k^m(\omega) = k_0^m + D^m(\Omega), \tag{41}$$

$$k_0^m = k^m(\omega_0) = k_0 + mk_{n0}, \tag{42}$$

and $k_{n0} = k_n(\omega_0)$. The Taylor expansion of the higher order terms is complex; therefore, the full expression for D^m will be determined below. Finally, we make a transformation to the envelope of the perturbation $\widetilde{v}_{x,y}$ by using

$$\widetilde{u}_{x,y} = \widetilde{v}_{x,y} e^{-ik_0' z}. \tag{43}$$

By means of Eqs.(36), (37), (38), and (39), the resulting first order wave equations are

$$\left[\partial_z + i\left(k'' - \frac{k_\perp^2}{2k''} - k_0'\right)\right]\widetilde{v}_x = -ik_n\widetilde{v}_{x(-)}^* \tag{44}$$

$$\left[\partial_z + i\left(k' - \frac{k_\perp^2}{2k'} - k_0'\right)\right]\widetilde{v}_y = -i\frac{k_n}{k^2}k_x k_y\left(\widetilde{v}_x + \widetilde{v}_{x(-)}^*\right). \tag{45}$$

2.4 Solving the Main Perturbation Equation

We first turn to a solution of Eq. (44); once $\widetilde{v}_x$ is known solution of Eq. (45) is straigthforward. In order to solve Eq. (44) we need an equation for $\widetilde{v}_{x(-)}^*$. This is obtained by taking the complex conjugate of Eq. (44) and by replacing $\Omega \to -\Omega$ in all Ω-dependent functions. In addition to $\widetilde{v}_x$ and $\widetilde{v}_{x(-)}^*$, $k(\omega)$, $k_n(\omega)$, and $n(\omega)$ also depend on Ω. In order to perform the sign inversion, k, k_n and n need to be split in even and odd parts that are symmetric and antisymmetric, respectively, with regard to sign change. We start with the

refractive index

$$n(\omega) = n(\omega_0 + \Omega) = n_0 + \Delta n(\Omega), \tag{46}$$

$$\Delta n(\Omega) = n(\omega) - n_0. \tag{47}$$

This can be split into even and odd components by defining

$$n_g(\Omega) = \frac{1}{2}\left(\Delta n(\Omega) + \Delta n(-\Omega)\right) \tag{48}$$

$$n_u(\Omega) = \frac{1}{2}\left(\Delta n(\Omega) - \Delta n(-\Omega)\right), \tag{49}$$

where $\Delta n(\Omega) = n_g(\Omega) + n_u(\Omega)$. The refractive indices $n_g(-\Omega) = n_g(\Omega)$ and $n_u(-\Omega) = -n_u(\Omega)$ fulfill the required sign inversion properties. Next we split

$$k = k_0 + D_g(\Omega) + D_u(\Omega) \text{ , with} \tag{50}$$

$$D_g = \frac{\omega_0}{c} n_g + \frac{\Omega}{c} n_u, \tag{51}$$

$$D_u = \frac{\omega_0}{c} n_u + \frac{\Omega}{c}\left(n_0 + n_g\right), \tag{52}$$

and $D(\Omega) = D_g + D_u$. The leading order terms of the even and odd dispersion functions are $D_g \approx (\beta_2/2)\Omega^2$ and $D_u \approx \beta_1\Omega$, respectively. Similarily, by means of $k_n = n_n\omega/\left(2cn(\Omega)\right) = n_n(\omega_0 + \Omega)/\left(2cn(\Omega)\right)$, the nonlinear wavevector is decomposed into

$$k_n = k_{n0} + D_n = k_{n0} + D_{ng}(\Omega) + D_{nu}(\Omega), \tag{53}$$

$$D_{ng} = \frac{n_0 k_{n0}}{n n_{(-)}}\left(n_g + n_u\overline{\Omega}\right), \tag{54}$$

$$D_{nu} = \frac{n_0 k_{n0}}{n n_{(-)}}\left(n_0\overline{\Omega} + n_g\overline{\Omega} - n_u\right), \tag{55}$$

where $k_{n0} = k_n(\omega_0)$, $D_n = D_{ng} + D_{nu}$, $n_{(-)} = n(-\Omega)$, and $\overline{\Omega} = \Omega/\omega_0$. We have approximated the first term to be $n_0^2 k_{n0}/(n n_{(-)}) = n_0^2 k_{n0}/((n_0 + n_g)^2 - n_u^2) \approx k_{n0}$ since $n_0 >> n_g$ and $n_0 >> n_u$. Finally by adding the linear and nonlinear contribution we obtain a general expression for $D^m = D + mD_n$ in Eq. (41), so

that k' and k'' are completely determined and seperable into even and odd parts, $D^m = D_g^m + D_u^m$ where $D_w^m = D_w + mD_{nw}$, with $w = g, u$ and $|^m = |', |''$ for $m = 1, 2$.

With the above definitions, the wave equation (44) and its complex conjugate equation become

$$\left[\partial_z + i\left(k_{n0} + D_g'' + D_u'' - \frac{k_\perp^2}{2k''}\right)\right]\widetilde{v}_x = -ik_n\widetilde{v}_{x(-)}^*, \tag{56}$$

$$\left[\partial_z - i\left(k_{n0} + D_g'' - D_u'' - \frac{k_\perp^2}{2k_{(-)}''}\right)\right]\widetilde{v}_{x(-)}^* = ik_{n(-)}\widetilde{v}_x, \tag{57}$$

with $k_{(-)}'' = k''(-\Omega)$ and $k_{n(-)} = k_n(-\Omega)$. Equation (57) has been obtained from (56) by complex conjugation, by replacing $\Omega \to -\Omega$, and by using the even and odd properties of the above defined functions of Ω. Equations (56) and (57) can be transformed into a second order equation for $\widetilde{v}_x$ alone by substituting for $\widetilde{v}_{x(-)}^*$,

$$\left[\partial_z + i\left(1 + \frac{k_\perp^2}{2k''k_{(-)}''}\right)D_u''\right]^2\widetilde{v}_x = \left[-\left(k_{n0} + D_g'' - \frac{k_\perp^2}{2k''k_{(-)}''}k_g''\right)^2 + k_nk_{n(-)}\right]\widetilde{v}_x, \tag{58}$$

where $k_g'' = k_0'' + D_g''$. Here we have used $1/k'' = k_{(-)}''/k''k_{(-)}''$, where $k_{(-)}'' = k''(-\Omega) = k_0'' + D_g'' - D_u''$ and $k''k_{(-)}'' = (k_0'' + D_g'')^2 - D_u''^2$. Equation (58) is in a form such that by inserting an exponential trial function, $\widetilde{v}_x \propto \exp(iK_zz)$, into Eq. (58) we obtain two wavevector solutions

$$K_z^\pm \equiv -K_u \pm K_g = -\left(1 + \frac{k_\perp^2}{2k''k_{(-)}''}\right)D_u'' \pm \left[\left(k_{n0} + D_g'' - \frac{k_\perp^2}{2k''k_{(-)}''}k_g''\right)^2 - k_nk_{n(-)}\right]^{1/2}, \tag{59}$$

where K_u and K_g are odd and even with respect to sign change $\Omega \to -\Omega$. There are two physically important situations. First, the perturbation field can grow out of noise, but as this is a complex undertaking on its own requiring quantum mechanical considerations; we leave it to be done in future work. Second, there is seeded growth, which we consider for the remainder of this work.

2.5 Seeded growth initial conditions

In the case of seeded growth, a general solution for $\widetilde{v}_x$ is given by

$$\widetilde{v}_x = \widetilde{d}_x^{+}(\mathbf{k}_\perp, \Omega) e^{iK_z^+ z} + \widetilde{d}_x^{-}(\mathbf{k}_\perp, \Omega) e^{iK_z^- z}, \tag{60}$$

where $\widetilde{d}_x^{+}$ and $\widetilde{d}_x^{-}$ are integration constants from the exponential solution. To determine these integration constants we need two independent quantities of the initial seed pulse. To proceed, we generate two equations by using the seed pulse initially, $\widetilde{v}_{x0} = \widetilde{v}_x(z=0)$, together with its first derivative, $\dot{\widetilde{v}}_{x0}$, just outside the Kerr material. In general this yields

$$\widetilde{v}_{x0} = \widetilde{d}_x^{+} + \widetilde{d}_x^{-}, \tag{61}$$

$$\dot{\widetilde{v}}_{x0} = iK_z^+ \widetilde{d}_x^{+} + iK_z^- \widetilde{d}_x^{-}. \tag{62}$$

From Eqs.(61) and (62) we obtain the two integration constants that are completely determined by the initial seed pulse and its derivative

$$\widetilde{d}_x^{\pm} = \frac{(K_g \pm K_u)\widetilde{v}_{x0} \mp i\dot{\widetilde{v}}_{x0}}{2K_g}\,. \tag{63}$$

Before we proceed by looking at the exponential growth regime of instability and solving for $\widetilde{v}_y$, it is instructive to test whether the result for the wavevector of the perturbation reduces to the well-known regimes of modulation instability and filamentation instability, as discussed in Chapter 1. This is a necessary test since our analysis is the spatio-temporal generalization of those regimes.

3 Limiting Cases of Modulation Instability and Filamentation Instability

We first look at the case of modulation instability which has been investigated for fibers in the 1D limit.

3.1 Modulation instability

In this case we have $k_\perp^2 = 0$. The treatment of modulation instability is limited to frequencies close to the center frequency, $\Omega << \omega_0$. In this limit, the frequency dependence of the nonlinear terms is negligible, $D_{nu} = D_{ng} \approx 0$, $D_g'' \approx D_g$, and $k_n k_{n(-)} \approx k_{n0}^2$. Furthermore, higher order dispersive terms can be neglected, i.e. $D_u \approx \beta_1 \Omega$ and $D_g \approx (\beta_2/2)\Omega^2$. Since D_u only appears in K_u it is simply a phase term that does not affect the instability. Upon returning to the time domain by an inverse Fourier transform, K_u simply results in putting the perturbation in a frame moving with the group velocity, $v_g \equiv 1/\beta_1$, such that we have the retarded time $\tau = t - \beta_1 z$. Finally, we have the correspondence $k_{n0} \iff \gamma P_0$ in fibers, with $\gamma = k_{n0}/A_{\text{eff}}$, where A_{eff} is the effective pulse area, and P_0 is the peak power[1]. Note that we have defined the total refractive index $(n^2 + n_n)$ differently to Ref.[1], where $n + n_n$ is used; this leads to a slightly different definition for the parameter γ. Using the above limits for the instability in Eq. (59) yields

$$\pm K_g \approx \pm \left([D_g + k_{n0}]^2 - k_{n0}^2 \right)^{1/2} \iff \pm \left(\left[\gamma P_0 + \frac{\beta_2}{2} \Omega^2 \right]^2 - (\gamma P_0)^2 \right)^{1/2}, \tag{64}$$

which is identical with the result derived for modulation instability[1].

3.2 Filamentation instability

The second limit of filamentation instability corresponds to the effect of nonlinear transverse diffusion at the center frequency. Thus, we let $\Omega \to 0$, for which $D''_u = 0 = D''_g$, $k_n = k_{n0}$, and $k''k''_{(-)} = (k_0 + 2k_{n0})^2$. Inserting these approximations in Eq.(59) gives

$$K_z^{\pm} \approx \pm \left(\left[k_{n0} - \frac{k_\perp^2}{2(k_0 + 2k_{n0})} \right]^2 - k_{n0}^2 \right)^{1/2} . \tag{65}$$

If $2k_{n0}/k_0 \ll 1$, which is true for most materials, provided $n_n \ll n^2$, then Eq.(65) reduces to

$$K_z^{\pm} \approx \pm \left(\left[k_{n0} - \frac{k_\perp^2}{2k_0} \right]^2 - k_{n0}^2 \right)^{1/2} , \tag{66}$$

which is equivalent to the results derived for filamentation instability[2].

Interestingly, the result in Eq.(65) shows that for light-matter interaction in highly Kerr-nonlinear materials, such as potassium titanyl phosphate (KTP)[3], then the filamentation instability regime should be corrected since then $k_0 + 2k_{n0} \approx k_0$ is no longer valid. To demonstrate this, we will obtain the maximum perpendicular wavevector by optimizing both Eqs.(65) and (66) to find the values of $\overline{k}_\perp^2 = k_{\perp max}^2$ in each case that correspond to maximum instability due to the arguments under the square roots being negative. Once these are obtained, we compare the magnitudes of each by inserting realistic numerical values for the parameters. That is, we want to solve for $\partial_{k_\perp^2} K_z^2 = 0$, and determine $\overline{k}_{\perp 1}^2$ and $\overline{k}_{\perp 2}^2$ corresponding to equations (65) and (66), respectively. We find

$$\overline{k}_{\perp 1}^2 = \frac{n_n k_0^2}{n^2} \left(1 + \frac{n_n}{n^2} \right) , \tag{67}$$

$$\overline{k}_{\perp 2}^2 = \frac{n_n k_0^2}{n^2} \tag{68}$$

In most materials $n_n/n^2 << 1$, so Eq.(68) is a very good approximation. This is different, however, for highly Kerr-nonlinear materials, like KTP. For example, operating at an intensity of $I_0 = 0.2$ GWcm^{-2} at $\lambda_0 = 800$nm we have $n = 1.75$[15], $n_2 = 2.54 \times 10^{-9}$ cm^{2}W^{-1}[3] so that $n_n = 0.59$ and thus $n_n/n^2 = 0.193$.

This translates to roughly a 19% difference between Eqs. (67) and (68), which is not negligible. Note that the above is valid in this analysis since we are in a regime that is still suitable for the Taylor expansion we made; namely $\sqrt{n^2+n_n} \approx n + n_n/(2n)$. We can prove this. Take

$$\frac{\sqrt{n_0^2+n_n}}{n_0+\frac{n_n}{2n_0}} = \frac{\sqrt{(1.75)^2+0.59}}{1.75+\frac{0.59}{2(1.75)}} = 0.9961, \tag{69}$$

and so the Taylor expansion is still valid, differing from the exact expression by less than 1%.

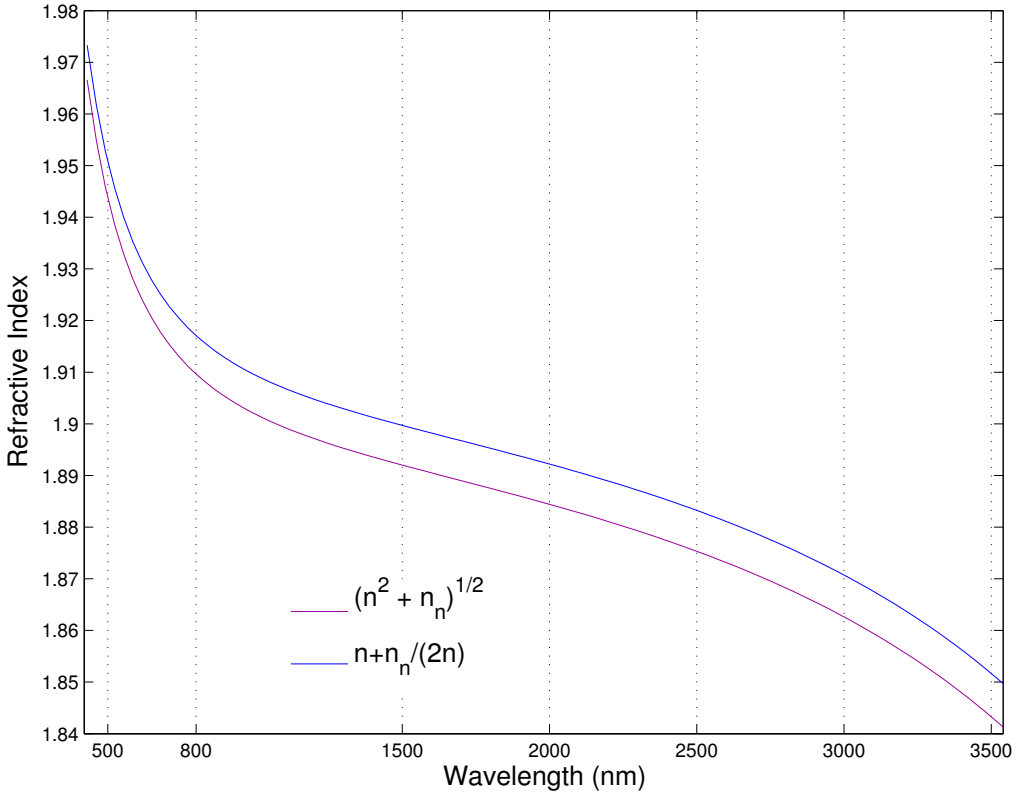

Figure 4: Comparing the total refractive index with and without Taylor expanding the refractive index for KTP with a source laser operating with an intensity of $I = 0.2$ GW/cm^2 at $\lambda_0 = 800$ nm. The linear refractive index data is taken from [16].

Furthermore, Fig. 4 demonstrates that the comparison made in Eq.(69) is valid over the entire range of wavelength data that we have. We can conclude that one should use Eq.(65) in the filamentation instability limit, especially for highly nonlinear materials, provided we respect the quantitative test outlined in Eq.(69). Let us now return to the general 3D analysis and explore the exponential growth regime of instability

corresponding to the general wavevector solution of Eq.(59).

4 Exponential growth regime of instability

4.1 Deriving the transverse wavevector corresponding to maximum KNI growth

As outlined in the last section, the second expression, K_g, in Eq. (59) contains a square root. When the argument of the square root is negative, this expression becomes imaginary resulting in an exponential growth or decay of the perturbation (60). This renders the initial plane wave solution $\mathbf{E}_0$ unstable. To identify the regime of instability, we calculate the values of $\mathbf{k}_{\perp 0}^2$ for which the expression under the square root gives zero, which results in

$$\begin{aligned}
\left[k_{n0} + D_g'' - \frac{k_\perp^2}{2k''k_{(-)}''}k_g''\right]^2 - k_n k_{n(-)} &= 0 \\
k_{n0} + D_g'' - \frac{k_\perp^2}{2k''k_{(-)}''}k_g'' &= \pm\sqrt{k_n k_{n(-)}} \\
\implies k_{\perp 0}^2 = \frac{2k''k_{(-)}''}{k_g''}\left(k_{n0} + D_g'' \pm \sqrt{k_n k_{n(-)}}\right) &. \qquad (70)
\end{aligned}$$

To identify the value of $k_\perp^2 = \overline{k}_\perp^2$ for which the growth of the KNI is maximum, we solve $\partial_{k_\perp^2} K_g^2 = 0$. This results in

$$\begin{aligned}
\frac{\mathrm{d}}{\mathrm{d}k_\perp^2}\left\{\left[k_{n0} + D_g'' - \frac{k_\perp^2}{2k''k_{(-)}''}k_g''\right]^2 - k_n k_{n(-)}\right\} &= 0 \\
-\frac{k_g''}{k''k_{(-)}''}\left[k_{n0} + D_g'' - \frac{k_\perp^2}{2k''k_{(-)}''}k_g''\right] &= 0 \\
\implies \overline{k}_\perp^2 = \frac{2k''k_{(-)}''}{k_g''}(k_{n0} + D_g'') &. \qquad (71)
\end{aligned}$$

In Section 2.3, the transverse components in Eqs.(38) and (39) were neglected because otherwise it makes the subsequent analysis significantly more complicated, without noticeable benefit. To prove this, we plot $\overline{k}_\perp$ for a material with high n_n for both cases of including and not including $k_\perp^2$ on the RHS and compare.

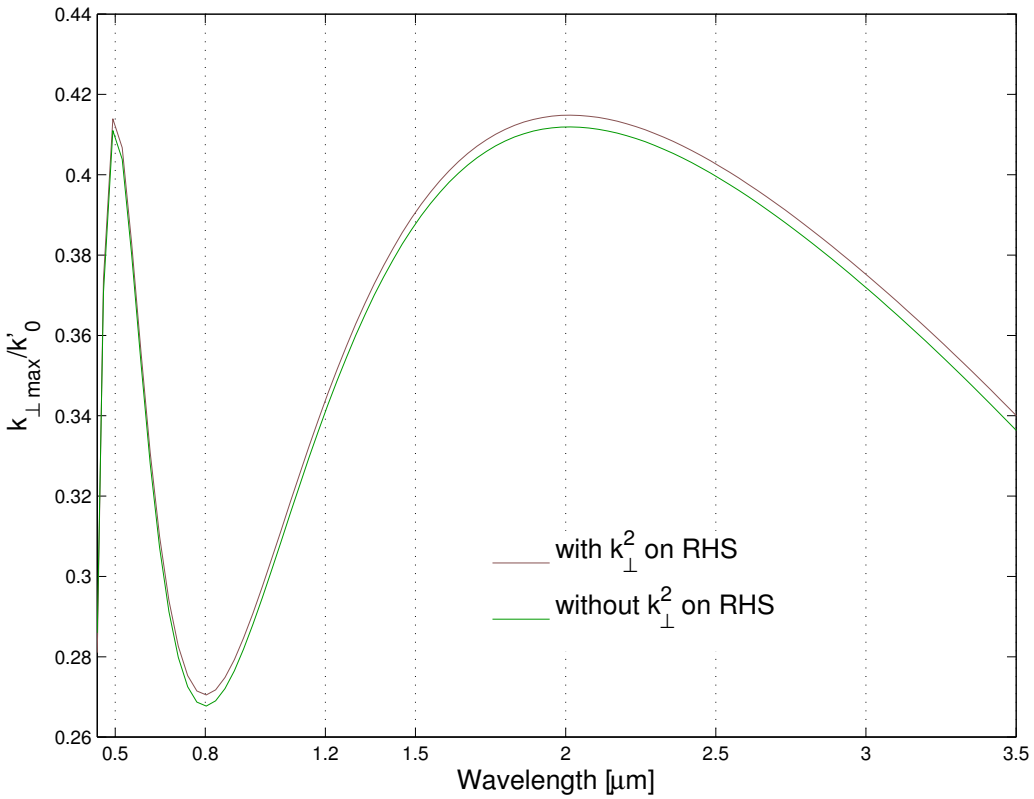

Figure 5: Comparing the transverse wavevector that corresponds to max growth with and without $k_\perp^2$ on the RHS of Eq.(38) for KTP at $\lambda_0 = 0.8\ \mu m$ for $n_n = 0.059$. The linear refractive index data is taken from [17].

It is evident in Fig. 5 that inclusion of the transverse components in Eqs.(38) and (39) yields negligible difference in the results provided $n_n \lesssim 0.06$. We can conclude that the transverse components on the RHS can be neglected when the leading order term is n_n, provided $n_n << n_0^2$.

By symmetry, the transverse wavevector corresponding to maximum growth, $\overline{\mathbf{k}}_\perp^2$, is located in the middle between the two transverse wavevectors, $\mathbf{k}_{\perp 0}^2$, for which $K_g = 0$. The half width over which exponential growth takes place is minimum and maximum points for which the interval in Eq.(70) is defined; namely,

$$\Delta_\perp^2 = \frac{2k''k''_{(-)}}{k''_g}\sqrt{k_n k_{n(-)}}\,. \tag{72}$$

The half width identifies the lower and upper bounds of the instability creating a cone of instability with $\overline{k}_\perp$ in the middle of this instability. Hence $\overline{k}_\perp$ corresponds to the cone emission angle and $\Delta_\perp$ will govern the

opening angle of the cone wherein instability can occur based on the coupling between $k_\perp$ and Ω.

4.2 Approximating the wavevector of the perturbation

In order to obtain a finite pulse shape in space and time, we make a Taylor expansion for small transverse momenta $k_\perp - \overline{k}_\perp$ such that $(k_\perp - \overline{k}_\perp)^p \approx 0$ for an integer $p > 2$. We insert $k_\perp = (k_\perp - \overline{k}_\perp) + \overline{k}_\perp$ into K_g of Eq.(59) with Eqs.(71) and (72).This results in

$$\begin{aligned}
K_g &= \left(\left[k_{n0} + D_g'' - \frac{\left((k_\perp - \overline{k}_\perp) + \overline{k}_\perp \right)^2}{2k''k''_{(-)}} k_g'' \right]^2 - k_n k_{n(-)} \right)^{1/2} \\
&= \left(\left[-\frac{(k_\perp - \overline{k}_\perp)^2 + 2\overline{k}_\perp (k_\perp - \overline{k}_\perp)}{2k''k''_{(-)}} k_g'' \right]^2 - k_n k_{n(-)} \right)^{1/2} \\
&\approx \left(\left[-\frac{\overline{k}_\perp (k_\perp - \overline{k}_\perp)}{k''k''_{(-)}} k_g'' \right]^2 - k_n k_{n(-)} \right)^{1/2} \\
&\approx i\sqrt{k_n k_{n(-)}} \left(1 - \frac{\left[\frac{\overline{k}_\perp (k_\perp - \overline{k}_\perp)}{k''k''_{(-)}} k_g'' \right]^2}{2k_n k_{n(-)}} \right) \\
\implies K_g &\approx \overline{K}_g \left[1 - 2\frac{\overline{k}_\perp^2 \left(k_\perp - \overline{k}_\perp \right)^2}{\Delta_\perp^4} \right].
\end{aligned} \tag{73}$$

The wavevector that corresponds to the maximum exponential amplitude gain is given by

$$\overline{K}_g = K_g(\overline{k}_\perp) = i\sqrt{k_n k_{n(-)}} = i\sqrt{\left(k_{n0} + D_{ng} \right)^2 - D_{nu}^2}\,.$$

Recall that we have used the transformation in Eq.(43). It will be useful, then, to define

$$K = k_0' + D_u'', \tag{74}$$

as the real part of the wavevector in the forward direction (not including the transverse component). Using this, we re-express K_u as

$$K_u = K - k_0' + \frac{D_u''}{2k''k_{(-)}''}k_\perp^2, \tag{75}$$

so that we have the Taylor-expanded full wavevector of the perturbation

$$K_z^- = -(K - k_0') - \overline{K}_g - ak_\perp^2 + ib\left(k_\perp - \overline{k}_\perp\right)^2, \tag{76}$$

where the following parameters have been defined

$$a = \frac{D_u''}{2k''k_{(-)}''}, \tag{77}$$

$$b = \frac{2\overline{K}_g\overline{k}_\perp^2}{\Delta_\perp^4} = \frac{2(k_{n0} + D_g'')}{\Delta_\perp^2}. \tag{78}$$

The expression for the wavevector in Eq.(76) is valid so long as we look at the transverse profile close to $\overline{k}_\perp$. It is useful for analyzing the optical KNI amplification by means of a seeded pulse because it provides a means to find an approximate closed-form of the pulse shape by means of transforming back to the space and time domain. This is explored in the next chapter.

5 Optical KNI Amplification

5.1 KNI amplification can outmatch absorption

Due to the exponential gain factor of the KNI, it can be used as an amplifier. Furthermore, the amplification will outmatch the absorption that arises due to the imaginary part of the linear refractive index[18], provided the intensity coupled with the nonlinear index, n_n, is high enough.

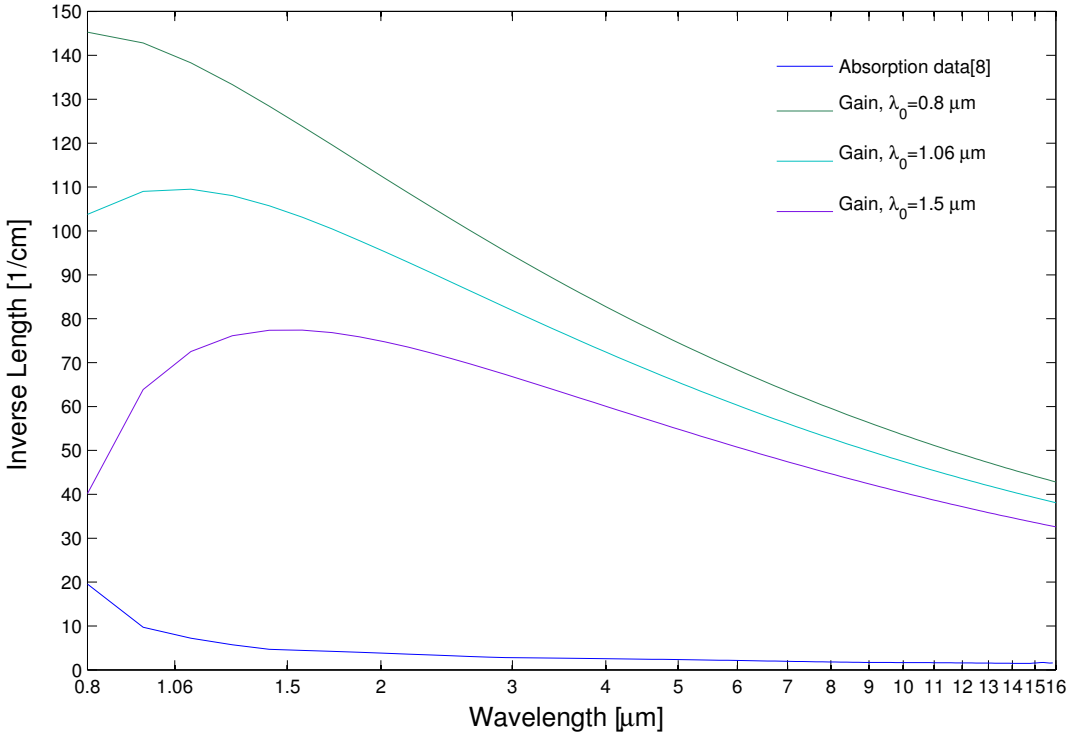

Figure 6: Comparing absorption to KNI amplification gain for $AgGaSe_2$ (AGSe), for a source operating at an intensity of $I = 1$ MWcm^{-2} at various center wavelengths. The nonlinear refractive index n_2 is taken from [3] to be $n_2 = 2.78 \times 10^{-9}$ cm^{2}W^{-1}. The linear refractive index data is taken from [19]; ordinary ray.

If we look at Fig. 6, the amplification clearly far outmatches the absorption of AGSe, even at a modest intensity. This is typically the case for nonlinear crystals. This applies for other materials as well, provided the intensity is high enough. This gives the assurance that it is feasible to attain KNI amplification in various materials, since it won't simply get overrun by absorption. Particularly for highly Kerr nonlinear materials that require a lower intensity to still attain a relatively high n_n. More importantly, we see the amplification is still strong into the mid (MIR) wavelength regimes, which constitutes wavelengths $\lambda \geq 3\mu$m[20]. Furthemore,

the plot shows that the amplification is still strong deep into the far infrared (FIR) wavelength regime, $\lambda \geq 8\mu$m[20]; the extent of our predictions are only limited by the available refractive index and absorption data for the given material[19],[8]. Achieveing an amplified laser at these wavelengths is an exciting endeavour, with many applications[21],[22]. To achieve FIR lasing without requiring population inversion in specific materials, such as organic compounds[23] is, to our knowledge, something that has not been achieved so far. As long as the dielectric has a high enough n_n such that the seed pulse interacts with the pump to achieve gain that outmatches the absorption at that wavelength, then amplification there is possible. Let's consider this in more detail with an example—a Gaussian seed pulse.

5.2 Gaussian seed pulse

For a Gaussian seed pulse, we start with Eq.(63) which corresponds to the integration constants that are determined by the initial conditions of the seed pulse. To determine the first derivative of the initial electric field at the surface of a nonlinear crystal, the scattering problem for the full wave equation (36) would need to be solved. Here we simplify this task by assuming that the pulse is propagating in an infinitely extended medium and that the nonlinearity is switched on at $z = 0$. Then the seed pulse can be described by a slowly varying pulse envelope, such as a Gaussian, with center frequency ω_1 and wavevector $k_1 = \omega_1 n_1/c$. Mathematically, the pulse would be described by[24]

$$\varepsilon_x(\mathbf{r}, z, t) = E_1 \frac{\mathrm{w}_0}{\mathrm{w}(z)} \exp\left(\frac{-r^2}{\widetilde{\mathrm{w}}(z)^2}\right) \exp\left(\frac{-t^2}{\widetilde{\tau}^2}\right) \exp\left[i\omega_1 t - ik_1 z + i\zeta(z)\right], \tag{79}$$

where E_1 is the initial amplitude of the pulse, w_0 is the beam waist, $r^2 = x^2 + y^2$ is the radius, t is time. The peak intensity, power and energy are defined by $I_1 = (2n_0/Z_0)E_1^2$, $P_1 = (\pi \mathrm{w}_0^2/2)I_1$ and $W_1 = (\pi/2)^{1/2} P_1 \tau$. The other parameters are defined by

$$\begin{aligned}
\frac{1}{\widetilde{\mathrm{w}}^2(z)} &= \frac{1}{\mathrm{w}^2(z)} + \frac{ik_1}{2R(z)}, & z_R &= \frac{k_1 \mathrm{w}_0^2}{2}, \\
\mathrm{w}(z) &= \mathrm{w}_0 \sqrt{1 + \frac{z^2}{z_R^2}}, & \frac{1}{\widetilde{\tau}^2} &= \frac{1}{\tau^2} + iC_t, \\
R(z) &= \frac{1}{z}\left(z^2 + z_R^2\right), & \zeta(z) &= \tan^{-1}\left(\frac{z}{z_R}\right),
\end{aligned} \tag{80}$$

where $\mathrm{w}(z)$ is the spot size as a function of propagation distance, z_R is the Rayleigh range, $R(z)$ is the radius of curvature, τ is the pulse duration, C_t is a quadratic temporal chirp, and $\zeta(z)$ is the Guoy phase shift. In order to determine $\dot{\widetilde{v}}_{x0}$ we need to take the Fourier transform of Eq.(79). First recall that $\varepsilon_x(\mathbf{r},z,t) = u_x(\mathbf{r},z,t)e^{i\omega_0 t}$ so that the time dependent components transform as

$$\hat{F}\left[u(t)\right] = \hat{F}\left[\varepsilon(t)e^{-i\omega_0 t}\right] = \frac{1}{\sqrt{2\pi}}\int_{-\infty}^{\infty} \mathrm{d}t\; e^{\frac{-t^2}{\widetilde{\tau}^2}} e^{i\omega_1 t} e^{-i\Omega t} = \frac{\widetilde{\tau}}{\sqrt{2}} \exp\left[-\frac{\widetilde{\tau}^2}{4}\left(\Omega-\omega_1\right)^2\right]. \tag{81}$$

The transverse components transform similarly as they are Gaussian as well. Furthermore, recall that $\widetilde{u}_x(\mathbf{k}_\perp,z,\Omega) = \widetilde{v}_x(\mathbf{k}_\perp,z,\Omega)e^{-ik_0' z}$. This means that we have

$$\widetilde{v}_x(\mathbf{k}_\perp,z,\Omega) = E_1 \frac{\widetilde{\tau}}{\sqrt{2}} \frac{\mathrm{w}_0 \widetilde{\mathrm{w}}(z)^2}{2\mathrm{w}(z)} \exp\left[-\frac{\widetilde{\tau}^2}{4}\left(\Omega-\omega_1\right)^2\right] \exp\left[-\frac{\widetilde{\mathrm{w}}(z)^2}{4}k_\perp^2\right] \exp[ik_0' z - ik_1 z + i\zeta(z)] \tag{82}$$

$$z \leq 0.$$

Taking the derivative with respect to z of Eq.(82) will allow us to fully specify the integration constants in Eq.(63). Since $R(z=0)=\infty$ and $\dot{\mathrm{w}}(z=0)=0$, taking the derivative and setting $z=0$ we have

$$\widetilde{v}_{x0} = E_1 \frac{\widetilde{\tau}}{\sqrt{2}} \frac{\mathrm{w}_0^2}{2} \exp\left(-\frac{\widetilde{\tau}^2}{4}\left(\Omega-\omega_1\right)^2\right) \exp\left(-\frac{\mathrm{w}_0^2}{4}k_\perp^2\right), \tag{83}$$

$$\dot{\widetilde{v}}_{x0} = i\left(k_0' - k_1 + \frac{1}{z_R}\right)\widetilde{v}_{x0}. \tag{84}$$

Inserting this into Eq.(63) we obtain

$$\widetilde{d}_x^{\pm} = d^{\pm}\widetilde{v}_{x0} = \frac{K_g \pm K_u \pm (k_0' - k_1 + \frac{1}{z_R})}{2K_g}\widetilde{v}_{x0}\,. \tag{85}$$

We are interested in the exponential growth regime with strong amplification, where the exponential solution corresponds to an optical KNI amplifier, meaning that only K_z^- is used since K_z^+ corresponds to evanescent decay and can be neglected. Further, we define $\overline{g} = -i\overline{K}_g = \sqrt{k_n k_{n(-)}}$ which is the maximum exponential

amplitude gain. Then, using Eqs.(60), (76) and (83)–(85) we obtain

$$\widetilde{u}_x \approx \overline{d}\exp\left[-\frac{\widetilde{\tau}^2}{4}\left(\Omega-\omega_1\right)^2\right]\exp\left[-\left(\frac{\mathrm{w}_0^2}{4}+iaz\right)k_\perp^2-bz(k_\perp-\overline{k}_\perp)^2\right]\exp[-iKz+\overline{g}z] \tag{86}$$

$$\overline{d} = E_1\frac{\widetilde{\tau}}{\sqrt{2}}\frac{\mathrm{w}_0^2}{2}d^-(\overline{k}_\perp) = E_1\frac{\widetilde{\tau}}{\sqrt{2}}\frac{\mathrm{w}_0^2}{2}\frac{1}{2\overline{K}_g}\left(\overline{K}_g-K-a\overline{k}_\perp^2+k_1-\frac{2}{k_1\mathrm{w}_0^2}\right). \tag{87}$$

5.3 Transforming back to the space domain

Since the electric field is centered around the maximum emission angle, we have approximated $k_\perp$ by $\overline{k}_\perp$ in the preexponential factor. To obtain the electric field of the amplified pulse in space and time, we must perform the inverse Fourier transform with regard to the transverse spatial coordinates and frequency. Starting with the transverse coordinates we have the following integral

$$I_\perp(z,r,\Omega) = \frac{1}{2\pi}\int_{-\infty}^{\infty}\int_{-\infty}^{\infty}\mathrm{d}k_x\mathrm{d}k_y\exp\left[-\left(\frac{\mathrm{w}_0^2}{4}+iaz\right)k_\perp^2-bz(k_\perp-\overline{k}_\perp)^2\right]e^{ik_xx}e^{ik_yy}. \tag{88}$$

Due to the radial symmetry, it is convenient to transform to cylindrical coordinates such that

$$\int_{-\infty}^{\infty}\int_{-\infty}^{\infty}\mathrm{d}k_x\mathrm{d}k_y \mapsto \int_0^{\infty}\int_0^{2\pi}k_\perp\mathrm{d}k_\perp\mathrm{d}\widetilde{\phi}.$$

Using the transformation in Eq.(88) results in

$$I_\perp(z,r,\Omega) = \frac{1}{2\pi}\int_0^{\infty}k_\perp\mathrm{d}k_\perp\exp\left[-\left(\frac{\mathrm{w}_0^2}{4}+iaz\right)k_\perp^2-bz(k_\perp-\overline{k}_\perp)^2\right]$$
$$\int_0^{2\pi}\mathrm{d}\widetilde{\phi}\exp\left[ik_\perp r\left(\cos\widetilde{\phi}\cos\phi+\sin\widetilde{\phi}\sin\phi\right)\right],$$

$$I_\perp(z,r,\Omega) = \int_0^{\infty}k_\perp\mathrm{d}k_\perp J_0(k_\perp r)\exp\left[-\left(\frac{\mathrm{w}_0^2}{4}+iaz\right)k_\perp^2-bz(k_\perp-\overline{k}_\perp)^2\right], \tag{89}$$

where $J_0(k_\perp r)$ is a Bessel function of the first-kind. For large enough $\overline{g}z$, the gain term dominates and we approximate the cross term $\exp\left(2bz\overline{k}_\perp k_\perp\right)$ in Eq.(89) by the leading order asymptotic expansion of the modified Bessel function $\exp(2bz\overline{k}_\perp k_\perp) \approx \overline{k}_\perp\sqrt{4\pi bz}I_0(2bz\overline{k}_\perp k_\perp)$. With that the integral (89) has the

solution [25]

$$I_\perp(z,r,\Omega) = \frac{\overline{k}_\perp\sqrt{\pi bz}}{b_z + iaz} e^{-h_1(z,\Omega)-ih_2(z,\Omega)} G_\perp(z,r,\Omega), \tag{90}$$

with

$$\begin{aligned} h_1(z,\Omega) &= \frac{\frac{\mathrm{w}_0^2}{4} bz\overline{k}_\perp^2}{b_z + iaz}\,, \;\; h_2(z,\Omega) = \frac{abz^2\overline{k}_\perp^2}{b_z + iaz}, \\ G_\perp(z,r,\Omega) &= J_0\left(\frac{bz\overline{k}_\perp r}{b_z + iaz}\right)\exp\left(-\frac{r^2}{4(b_z + iaz)}\right), \end{aligned} \tag{91}$$

and with $b_z = bz + \mathrm{w}_0^2/4$. The radial beam profile is a product of a Bessel beam and Gaussian beam. Asymptotically for $z \to \infty$ the radial profile becomes a complex Bessel beam, $J_0\left(bz\overline{k}_\perp r/(b_z + iaz)\right) \approx J_0\left[\overline{k}_\perp r/(1 + ia/b)\right]$. By using Eqs.(86), (87), (90), and (91) we obtain the electric field of the perturbation in real space as a function of frequency,

$$\begin{aligned} \widetilde{u}_x(z,r,\Omega) &= f(z,\Omega)e^{-h_1(z,\Omega)+\overline{g}(\Omega)z} G_\perp(z,r,\Omega) e^{-\frac{\tilde{\tau}^2}{4}(\Omega-\omega_1)^2} e^{-iK(\Omega)z - ih_2(z,\Omega)}, \\ f(z,\Omega) &= \sqrt{\pi bz}\frac{\overline{d}\;\overline{k}_\perp}{b_z + iaz}\,. \end{aligned} \tag{92}$$

In addition, $a(\Omega)$, $b(\Omega)$, and $\overline{k}_\perp(\Omega)$ depend on Ω. We want to consolidate the exponential terms in Eq.(92) and split into real and imaginary parts so that we can differentiate between phase terms that modify the electric field versus real terms that will affect the intensity profile of the perturbation during amplification. For that we look at the functions $h_1(z,\Omega)$ and $h_2(z,\Omega)$ and split them into real and imaginary parts by rationalizing the denominator to obtain

$$h_1(z,\Omega) = \frac{\frac{\mathrm{w}_0^2}{4} bz\overline{k}_\perp^2}{b_z + iaz} = \frac{\frac{\mathrm{w}_0^2}{4} bz\overline{k}_\perp^2\,(b_z - iaz)}{b_z^2 + a^2z^2}, \tag{93}$$

$$ih_2(z,\Omega) = i\frac{abz^2\overline{k}_\perp^2}{b_z + iaz} = i\frac{abz^2\overline{k}_\perp^2\,(b_z - iaz)}{b_z^2 + a^2z^2}. \tag{94}$$

Combining the real and imaginary parts of h_1 and h_2 serparately and splitting $K(\Omega) = D_u'' + k_0'$ we obtain

$$\eta(z,\Omega) \equiv \frac{bz\left(\frac{\mathrm{w}_0^2}{4}b_z + a^2z^2\right)\overline{k}_\perp^2}{b_z^2 + a^2z^2},$$
$$i\phi(z,\Omega) \equiv i\frac{ab^2z^3\overline{k}_\perp^2}{b_z^2 + a^2z^2} + iD_u''z. \tag{95}$$

Notice that since ϕ contains odd functions of Ω, then $(i\phi)^* = -i(-\phi) = i\phi$. Thus, it is a phase term with frequency components that do not become negative upon conjugation. Using this in (92) we obtain a more physically intuitive form of the solution, namely

$$\widetilde{u}_x(z,r,\Omega) = f(z,\Omega)e^{\overline{g}(\Omega)z - \eta(z,\Omega) - i\phi(z,\Omega)}G_\perp(z,r,\Omega)e^{-\frac{\widetilde{\tau}^2}{4}(\Omega-\omega_1)^2}e^{-ik_0'z}. \tag{96}$$

Since amplification is desired, we want to be in a regime where $\eta(z,\Omega)$ does not wash out the effects of the gain given by $\overline{g}z$. As $k_0 \gg \overline{g}$, we find that $a/b \approx -\overline{g}D_u/(2k_0D_g) \ll 1$. This implies that the complex Bessel beam can be Taylor expanded to first order. Further, in the limit of strong amplification, $b_z \approx bz$. We also assume that the initial seed spectrum does not change much over $\Delta_\perp$, so that frequency depenedence in $\eta(z,\Omega)$ can be neglected, i.e. $\overline{k}_\perp^2(\Omega) \approx \overline{k}_\perp^2(\Delta\omega)$, where $\Delta\omega \equiv \omega_1 - \omega_0$. Finally, in the pre-exponential factor the frequency dependence is also neglected, $f(\Omega) \approx f(\Delta\omega)$. Recall as well that $a + D_u'' = D_u''\left(1 + 1/2k''k_{(-)}''\right)$. As a result, the following terms in Eq. (92) can be simplified to

$$\eta(z,\Omega) \approx \left[\frac{\mathrm{w}_0^2}{4}\overline{k}_\perp^2\right](\Delta\omega), \quad \phi(z,\Omega) \approx D_u''\left[\left(1 + \frac{\overline{k}_\perp^2}{2k''k_{(-)}''}\right)z\right](\Omega), \tag{97}$$
$$f(z,\Omega) \approx \left[\sqrt{\frac{\pi}{bz}}\overline{k}_\perp\overline{d}\right](\Delta\omega), \quad G_\perp(z,r,\Omega) \approx \left(J_0\left(\overline{k}_\perp(\Omega)r\right) + i\frac{az}{b_z}\overline{k}_\perp(\Omega)rJ_1\left(\overline{k}_\perp(\Omega)r\right)\right)\exp\left(-\frac{r^2}{4b(\Omega)z}\right),$$

where $J_1(\xi)$ is a first-order Bessel function of the first kind. We further assume that az is small enough so that the J_1 term can be neglected compared to the J_0 contribution. Then, with the above simplifications, one obtains

$$\widetilde{u}_x(z,r,\Omega) \approx f(z,\Delta\omega)e^{-\eta(\Delta\omega)-i\phi(z,\Omega)}e^{\overline{g}(\Omega)z}J_0\left(\overline{k}_\perp(\Omega)r\right)\exp\left(-\frac{r^2}{4b(\Omega)z}\right)\exp\left[-\frac{\widetilde{\tau}^2}{4}(\Omega-\omega_1)^2\right]e^{-ik_0'z}. \tag{98}$$

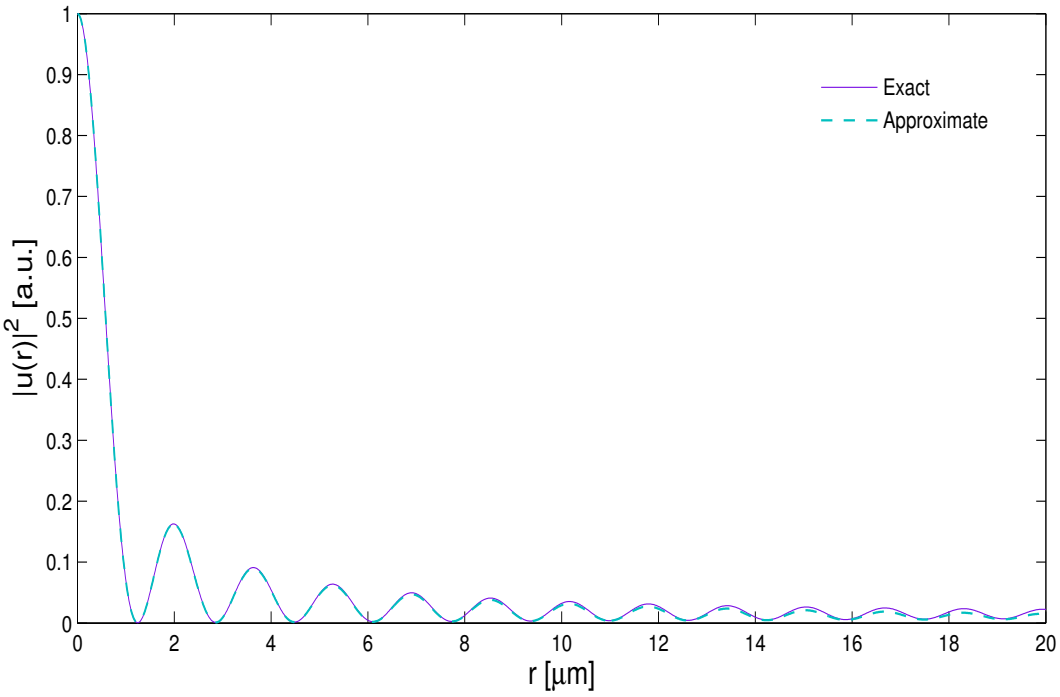

Figure 7: Numerical comparison of the exact and approximate radial intensity profiles for KTP with $\lambda_0 = 0.8$ μm, $\lambda_1 = 3$ μm, $I_0 = 3$ MW/cm^2, $z = 10/\bar{g}$, and $|az/b_z| = 0.0168$. The linear refractive index data is taken from [17].

In Fig. 7 numerical comparison shows that for $|az/b_z| \leq 0.017$ the approximation reproduces the exact expressions almost perfectly. Thus, we want strong amplification, but to still respect the restriction $k_0 >> \bar{g}$. This renders η to be a constant phase term and hence will not scramble the signal during amplification. We also want η to be small. Quantitatively, this means that we want

$$\eta = \frac{\mathrm{w}_0^2 \bar{k}_\perp^2}{4} \lesssim 1 \implies \mathrm{w}_0 \lesssim \frac{2}{\bar{k}_\perp}. \tag{99}$$

This imposes a condition on a controllable parameter, that of the width of the seed pulse. As well, strong amplification can be quantified as meaning that $\bar{g}z \geq 10$ since this results in an amplification of the perturbation field by over 4 orders of magnitude. This means that we want a propagation distance of

$$z \geq \frac{10}{\bar{g}}. \tag{100}$$

Clearly, the higher the intensity of the pump, the larger $\overline{g}$ is, and hence we require a shorter propagation distance. Furthermore, if a is small compared to b, then this coincides with D_u'' being relatively small as well. This means that the chirping that results from ϕ will be small and the amplification won't be noticeably impeded by the odd dispersive terms of D_u''. Quantitatively, looking at ϕ and using $z \geq 10/\overline{g}$ we have

$$D_u''\left(1+\frac{\overline{k}_\perp^2}{2k''k''_{(-)}}\right)\left(\frac{10}{\overline{g}}\right) \lesssim 1 \implies D_u'' \lesssim \frac{\overline{g}}{10\left(1+\frac{\overline{k}_\perp^2}{2k''k''_{(-)}}\right)}. \tag{101}$$

Under these assumptions outlined above, then, we have the simplified form of the perturbation within a parameter space such that amplification can occur unhindered. The next step is to use the simplified form of the perturbation in transforming back to the time domain.

5.4 Transforming from the frequency domain to the time domain

In order to transform back to the time domain, we introduce a new freqency Ω_1 centered around ω_1 by noting that $\Omega = \omega - \omega_1 + \omega_1 - \omega_0 = \Omega_1 + \Delta\omega$. Spatio-temporal coupling is determined by the frequency dependence of b and $\overline{k}_\perp$, which determine the spatial extent of the Bessel beam. To keep the notation manageable, we define the following phase term

$$\Phi(z,r,\Omega) \equiv \overline{g}(\Omega) - i\phi(z,\Omega) - \frac{r^2}{4b(\Omega)z}.$$

Using this together with the fact that $\varepsilon_x = u_x e^{i\omega_0 t} = \hat{F}^{-1}\left[\widetilde{u}_x\right] e^{i\omega_0 t}$ in Eq.(98) and

$$\int_{-\infty}^{\infty} \mathrm{d}\omega\ e^{i\omega t} = \int_{-\infty}^{\infty} \mathrm{d}\Omega_1\ e^{i\Omega_1 t} e^{i\omega_1 t},$$

gives us the perturbation field in space and time as

$$\epsilon_x(z,r,t) = f(z,\Delta\omega)e^{-\eta(\Delta\omega)} \exp\left[i\omega_0 t + i\omega_1 t - k_0' z\right] e^{\Phi(z,r,\Delta\omega)} I(z,r,t), \tag{102}$$

$$I(z,r,t) = \frac{1}{\sqrt{2\pi}}\int_{-\infty}^{\infty} d\Omega_1 e^{i\Omega_1 t} e^{-\frac{\tilde{\tau}^2}{4}(\Omega_1-\omega_0)^2} J_0\left[\overline{k}_\perp(\Delta\omega+\Omega_1)r\right] \exp\left[\Phi(z,r,\Delta\omega+\Omega_1) - \Phi(z,r,\Delta\omega)\right]. \tag{103}$$

In general, the linear refractive index in closed form as a function of frequency is unknown. It may be approximated for a specific material using a Sellmeier formula[1] and then Eq.(103) can be solved approximately. However, for a more general analytical solution that is not dependent on one specific material only, one must treat Ω_1 as small, and then expand Φ_t to second order and $\overline{k}_\perp$ to first order in Ω_1 to obtain leading order even and odd terms of group velocity and group velocity dispersion, respectively. As the result is very involved, it is left for future work.

6 Conclusion

6.1 Summary and results

To summarize, one of the reasons why lasers are interesting is their capacity for high intensity. The Kerr nonlinearity that manifests through the third order term of the polarization vector is very small in most materials, but is intensity-dependent[3]. Thus, it becomes relevant for lasers. This results in a nonlinear intensity dependent refractive index that has many interesting consequences for nonlinear optics.

This work is a perturbative spatio-temporal analysis that starts from Maxwell's equations and its constituent relations to derive a nonlinear wave equation. The equation is linearized in the perturbation, $\boldsymbol{\varepsilon}$, assuming it is small compared to the driving electric field. This approximation limits one to observe the onset of nonlinear effects, but once $\mathcal{O}(\boldsymbol{\varepsilon}^2) \approx 0$ is no longer valid, the analysis is insufficient. Many of the mathematical details were included in the derivation to demonstrate that this is an alternative method of studying the theory of spatio-temporal Kerr nonlinear optics that differs from the usual approach of using the Nonlinear Schrödinger Equation[1] or nonlinear transverse diffusion equation[2]. The exponential wavevector solution was a generalization to modulation and filamentation instability, and we saw in Chapter 3 that it behaved correctly in the respective limiting cases.

Further, by solving the general wavevector solution (Eq. (59)), there is also the prediction of KNI amplification. This directly results from the perturbation being coupled with its complex conjugate. The solution yields an instability regime where the wavevector becomes complex, resulting in exponential growth. Thus, treating the perturbation as a small seed pulse can interact with a pump pulse in a nonlinear dielectric medium and be amplified to the order of the pump intensity and even far beyond, with required propagation lengths easily attainable in an experiment (see Fig. 6). Incredibly, wavelengths that are typically hard to have a laser signal, such as deep into the infrared can be amplified and it does not involve inverting the population of the material. Exploring KNI amplification and other aspects of KNI theory will be the subject of future work.

6.2 Future work

The analysis that was done in this work laid the foundation for future endeavours. For example, Future work can include generalizing the ansatz so that the pump laser is finite in both space and time, resulting in a more realistic solution to the instability analysis, with the spatial and temporal widths of the pump laser playing a quantitative role in determining a scheme for amplification. Furthermore, the intensity of the driving field becomes dependent on space and time, directly incorporating self-focusing and SPM physics into the driving laser. This, along with allowing for non-collinearity between the pump and seed pulses will allow for better collaboration with experiments that are currently being done on KNI.

Going beyond the linearized perturbation could also be beneficial to describe more than just the onset of effects. As mentioned in the conclusion, it was assumed that the perturbation was small. However, in the case of the perturbation growing by means of KNI instability, we must go beyond the linearized equations if we want to describe the effects that arise when the perturbation is on the order of the pump pulse or greater.

The analysis done in Chapter 5 to find a closed-form solution for $\varepsilon(r, z, t)$ can be taken further to solve Eq.(103) by assuming small frequency shift away from center, and Taylor expanding the odd and even dispersion terms to first and second order, respectively.

It is pertinent to investigate conical emission and supercontinuum generation as these are also Kerr nonlinear optical effects, and their origins are still debated. If the theory behind these effects were established by means of KNI, it would further reinforce the usefulness of the theory.

Free electron ionization can be introduced into the nonlinear wave equation. In the strong field regime this inclusion becomes important, and so it is worthwhile to perform the KNI analysis with this plasma defocusing term[26].

Solving the perturbation equation that is $\hat{y}$-polarized (Eq.(45)) is potentially important. Since the $\hat{y}$-polarized perturbation grows out of the $\hat{x}$-polarized perturbation, then by comparing the ratio of their intensities, in principal, one could measure the nonlinear index of refraction in an experiment.

Another endeavour could be to repeat the analysis for exotic materials in which $n \leq 0$, where n is the linear refractive index. This renders the assumption that the asymmetry between transverse components cannot be neglected, as was done in Chapter 2. Furthermore, it would no longer be valid to assume that we

could Taylor expand the full wavevectors k' and k'' in the same way when we split the frequency-dependent functions into even and odd components. This would alter the analysis and could yield potentially interesting results.

It would also be interesting to look at different cases for the perturbation itself. It was mentioned that the perturbation could be treated as noise arising from vacuum flucuations, but this is inherently a quantum mechanical problem that requires careful consideration. Namely, quantizing the electric field by means of the quantum harmonic oscillator treatment wherein the zero-point energy of the potential well corresponds to the vacuum flucuations. This is a complex undertaking but the analysis will describe how the Kerr nonlinearity acts on the noise quantitatively. This could potentially have important implications, i.e. if there is a noticeable interaction between vacuum flucuations and a seed pulse. In any case, it's always beneficial to understand the noise better, because it is a natural phenomenon that has an impact on laser physics.

In the case of the perturbation being a seed pulse, other beam profiles aside from Gaussian could also be incorporated into the amplification analysis. For instance, one could use a Bessel beam as the seed pulse which may prove to be a natural choice due to the radial symmetry of the transverse components of the wavevector. This radial symmetry yields a Bessel function when transforming back to space coordinates. Due to the spatio-temporal coupling this also yield a Bessel function when transforming back to the time domain as well. Hence, it could simplify the analysis to treat the perturbation as a Bessel beam in the first place.

This thesis has opened the door for much more work to be done in the field of Nonlinear Optics. Currently, a manuscript extending KNI in some of ways mentioned above is being prepared. It has been my privilege to contribute to this endeavour, and I am eager to keep working in this field.

References

[1] G. P. Agrawal, *Nonlinear Fiber Optics*, Academic Press, San Diego (1989).

[2] V. I. Bespalov and V. I. Talanov, JETP Lett. 3, 307 (1966).

[3] R. W. Boyd, *Nonlinear Optics*, third edition, Academic Press, San Diego (2003).

[4] RP Photonics Encyclopedia, https://www.rp-photonics.com/pockels_cells.html

[5] M. Melnichuk, L.T. Wood, Phys. Rev. A 82, 013821 (2010).

[6] Stolen, R.; Lin, C. (April 1978). "Self-phase-modulation in silica optical fibers". Phys. Rev. A 17 (4): 1448–1453.

[7] Cumberbatch, E. "Self-focusing in Non-linear optics", J. Inst. Maths Applics 6, 250 (1970).

[8] RP Photonics Encylopedia, https://www.rp-photonics.com/optical_intensity.html

[9] Chin, S.L.; Wang, T.J.; Marceau, C., JOSA B, 31, 2, 321 (2014).

[10] RP Photonics Encylopedia, https://www.rp-photonics.com/solitons.html

[11] Hercher, M. JOSA A 54, 563 (1964).

[12] Refractive Index Database, http://refractiveindex.info/?shelf=mainbook=AgGaSe2

[13] Wolfram Mathworld, http://mathworld.wolfram.com/ConvolutionTheorem.html

[14] T. Brabec and F. Krausz, Phys. Rev. Lett. 78, 3282 (1997).

[15] P. Schiebener, J. Straub, J. M. H. Levelt Sengers, and J. S. Gallagher, J. Phys. Chem. 19, 677 (1990).

[16] P. E. Ciddor, Appl. Opt. 35, 9, 1566 (1996).

[17] K. Kato and E. Takaoka, Appl. Opt. 41, 5040 (2002).

[18] University of Reading, https://www.reading.ac.uk/infrared/library/substrateopticaltheory/ir-substrateopticaltheory-absorptionandextinctioncoefficienttheory.aspx

[19] A. Harasaki and K. Kato, Jpn. J. Appl. Phys. 36, 700 (1997).

[20] RP Photonics Encyclopedia, https://www.rp-photonics.com/infrared_light.html

[21] IPG Photonics, http://www.ipgphotonics.com/Mid_ir_lasers.htm

[22] US National Library of Medicine, National Institutes of Health, http://www.ncbi.nlm.nih.gov/pmc/articles/PMC3699878/

[23] M. Csele, *Fundamentals of Light Sources and Lasers*, first edition, John Wiley Sons, New York (2004).

[24] A. Yariv, *Quantum Electronics*, third edition, John Wiley Sons, New York (1988).

[25] I. S. Gradshteyn and I. M. Ryzhik, *Table of Integrals, Series, and Products*, seventh edition, Academic Press, Burlington (2007).

[26] M. Geissler, G. Tempea, A. Scrinzi, M. Schnürer, F. Krausz, and T. Brabec, Phys. Rev. Lett. 83, 2930 (1999).

[27] RP Photonics Encyclopedia, https://www.rp-photonics.com/supercontinuum.html

[28] M. Kolesik, E. M. Wright, and J.V. Moloney, Opt. Lett. 35, 15, 2550 (2010).

[29] K. D. Moll, A. L. Gaeta, and G. Fibich, Phys. Rev. Lett. 90, 203902 (2003).